Accepted Manuscript

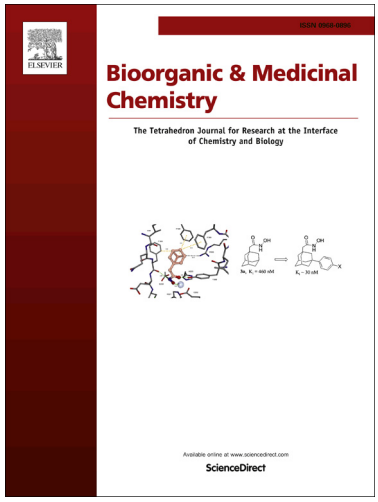

Optimization of a Novel Series of *N*-Phenylindoline-5-sulfonamide-based Acyl CoA:Monoacylglycerol Acyltransferase-2 Inhibitors: Mitigation of CYP3A4 Time-dependent Inhibition and Phototoxic Liabilities

Kenjiro Sato, Hiroki Takahagi, Osamu Kubo, Kousuke Hidaka, Takeshi Yoshikawa, Masahiro Kamaura, Masanori Nakakariya, Nobuyuki Amano, Ryutaro Adachi, Toshiyuki Maki, Kazumi Take, Shiro Takekawa, Tomoyuki Kitazaki, Tsuyoshi Maekawa

PII: S0968-0896(15)00497-6
DOI: http://dx.doi.org/10.1016/j.bmc.2015.06.003
Reference: BMC 12359

To appear in: *Bioorganic & Medicinal Chemistry*

Received Date: 24 April 2015
Revised Date: 1 June 2015
Accepted Date: 2 June 2015

Please cite this article as: Sato, K., Takahagi, H., Kubo, O., Hidaka, K., Yoshikawa, T., Kamaura, M., Nakakariya, M., Amano, N., Adachi, R., Maki, T., Take, K., Takekawa, S., Kitazaki, T., Maekawa, T., Optimization of a Novel Series of *N*-Phenylindoline-5-sulfonamide-based Acyl CoA:Monoacylglycerol Acyltransferase-2 Inhibitors: Mitigation of CYP3A4 Time-dependent Inhibition and Phototoxic Liabilities, *Bioorganic & Medicinal Chemistry* (2015), doi: http://dx.doi.org/10.1016/j.bmc.2015.06.003

Optimization of a Novel Series of *N*-Phenylindoline-5-sulfonamide-based Acyl CoA:Monoacylglycerol Acyltransferase-2 Inhibitors: Mitigation of CYP3A4 Time-dependent Inhibition and Phototoxic Liabilities

Kenjiro Sato, Hiroki Takahagi, Osamu Kubo, Kousuke Hidaka, Takeshi Yoshikawa, Masahiro Kamaura, Masanori Nakakariya, Nobuyuki Amano, Ryutaro Adachi, Toshiyuki Maki, Kazumi Take, Shiro Takekawa, Tomoyuki Kitazaki, and Tsuyoshi Maekawa*

Pharmaceutical Research Division, Takeda Pharmaceutical Co., Ltd., 26-1, Muraoka-Higashi 2-Chome, Fujisawa, Kanagawa 251-8555, Japan

*Corresponding author; Phone: +81 466 32 1072; Fax: +81 466 29 4475;

E-mail: kenjirou.satou@takeda.com

Abstract

Acyl CoA:monoacylglycerol acyltransferase-2 (MGAT2) has emerged as a potential peripheral target for the treatment of obesity and metabolic disorders. We previously identified a novel series of *N*-phenylindoline-5-sulfonamide derivatives exemplified by **2** as potent and orally bioavailable MGAT2 inhibitors. Despite its attractive potency, further assessment revealed that this compound exhibited time-dependent inhibition (TDI) of cytochrome P450 3A4 (CYP3A4). To remove the undesirable CYP3A4 TDI activity, structural modification was focused on the 2,4-difluoroaniline moiety on the basis of the assumption that this moiety would be involved in mechanism-based inhibition of CYP3A4 via oxidative metabolism. This led to the finding that the introduction of 4-chloro-2,6-difluoroaniline significantly improved CYP3A4 TDI risk. Further optimization resulted in the discovery of *N*-(4-chloro-2,6-difluorophenyl)-1-{5-[1-methyl-3-(trifluoromethyl)-1*H*-pyrazol-5-yl]pyrimidin-2-yl}-7-(2-oxopyrrolidin-1-yl)-2,3-dihydro-1*H*-indole-5-sulfonamide (**27c**) with potent MGAT2 inhibitory activity (IC_{50} = 7.8 nM) and excellent ADME-Tox profiles including metabolic stability, oral bioavailability, and CYP3A4 TDI. In a mouse oral fat tolerance test, compound **27c** effectively and dose-dependently suppressed the elevation of plasma triacylglycerol levels after oral administration at doses of 1 and 3 mg/kg. We also discuss mitigation of the phototoxic liability of biaryl derivatives on the basis of the HOMO–LUMO gap hypothesis during the course of optimization efforts.

Keywords

MGAT2 inhibitor, acyltransferase, triacylglycerol, obesity, metabolic disease, indoline, time-dependent inhibition, CYP3A4, phototoxicity

Abbreviations

ACAT, acyl CoA:cholesterol acyltransferase; ADME, absorption, distribution, metabolism and excretion; APCI, atomospheric pressure cheimcal ionization; CM, chylomicron; dba, dibenzylideneacetone; CYP, cytochrome P450; DDI, drug–drug interaction; DGAT, acyl CoA:diacylglycerol acyltransferase; DIEA, *N*,*N*-diisopropylethylamine; DMPK, drug metabolism and pharmacokinetics; HOMO, highest occupied molecular orbital; HLM, human liver microsome; LLE, ligand lipophilicity efficiency; LPL, lipoprotein lipase; LUMO, lowest unoccupied molecular orbital; MGAT, acyl CoA:monoacylglycerol acyltransferase; MLM, mouse liver microsome; MRT, mean residence time; OFTT, oral fat tolerance test; TEA, triethylamine; TDI, time-dependent inhibition ; TG, triacylglycerol.

Graphical Abstract

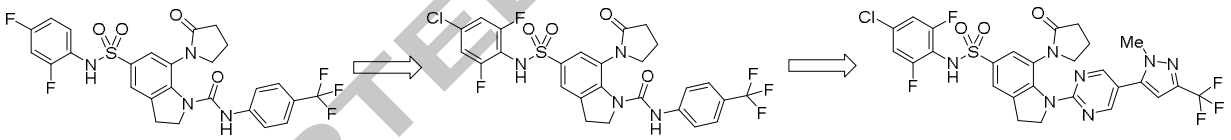

2
hMGAT2 IC_{50} = 3.4 nM
$LogD_{7.4}$ = 3.1
potenitial CYP3A4 TDI risk

9a
hMGAT2 IC_{50} = 30 nM
$LogD_{7.4}$ = 3.3
low CYP3A4 TDI risk

27c
hMGAT2 IC_{50} = 7.8 nM
$LogD_{7.4}$ = 2.8
low CYP3A4 TDI risk
BA 50% (mouse, 1 mg/kg)

1. Introduction

Triacylglycerol (TG) constitutes a major class of neutral lipids and serves as an essential form of energy storage in the human body. TG also plays an important role as a carrier of fatty acids to peripheral tissues. However, excess storage of TG in adipose and nonadipose tissues causes various pathological conditions such as obesity, insulin resistance, dyslipidemia, and hepatic steatosis.[1, 2] In addition, several studies have indicated that TG-rich lipoproteins are an independent risk factor for cardiovascular disease.[3-5] Therefore, an appropriate modulation strategy for TG metabolism is expected to restore abnormally elevated levels of TG and improve TG-related cardiometabolic disorders.

One potential therapeutic approach is to inhibit the biosynthesis of TG. Acyl CoA:monoacylglycerol acyltransferase-2 (MGAT2) is a member of the DGAT2 gene family of enzymes and catalyzes the synthesis of diacylglycerol from monoacylglycerol and fatty acyl CoA, which is a crucial step in TG synthesis by the MGAT pathway.[6, 7] This enzyme is highly expressed in the intestine and is considered to play an important role in dietary fat absorption. Recent research demonstrated that MGAT2 gene knockout mice were resistant to olive oil-induced hypertriglyceridemia, high-fat induced obesity, and metabolic disorders such as insulin resistance, hypercholesterolemia, and fatty livers.[8-10] Interestingly, the MGAT2-deficient mice displayed higher energy expenditure than the wild-type mice. These preclinical data highlight that MGAT2 is critically involved in fat absorption as well as energy metabolism, suggesting that the inhibition of MGAT2 could serve as a novel peripheral target for the treatment of obesity and metabolic disorders. Furthermore, the facts that the MGAT2-deficient mice normally gained weight on a low-fat diet and displayed no apparent abnormalities, including fatty stool, would warrant the safety profile of MGAT2 inhibitors.

Till date, several chemical classes of MGAT2 inhibitors have been identified;[11, 12] however, there have been no clinical studies using MGAT2 inhibitors. We previously reported the discovery of a novel series of *N*-phenylindoline-5-sulfonamide derivatives as potent, selective, and orally bioavailable MGAT2 inhibitors, as exemplified by **2** (Figure 1).[13] Compound **2** exhibited potent MGAT2 inhibitory activity and suppressed the elevation of TG in a mouse oral fat tolerance test (OFTT) after oral administration. These attractive profiles motivated us to evaluate this compound in detail in terms of drug–drug interactions (DDIs) and toxicity profiles. Unfortunately, compound **2** exhibited time-dependent inhibition (TDI) of cytochrome P450 3A4 (CYP3A4). Because CYP3A4 is the most abundant CYP isoform and is responsible for the oxidative metabolism of a wide variety of clinical drugs, TDI of this metabolizing enzyme may preclude the drug development of compounds from the perspective of DDIs.[14] Accordingly, our subsequent optimization effort was directed toward addressing the CYP3A4 TDI issue to produce a clinical candidate with safe profiles. In this paper, we report the design, synthesis, and biological evaluation of *N*-phenylindoline-5-sulfonamide derivatives as novel MGAT2 inhibitors, which led to the identification of compound **27c** with potent MGAT2 inhibitory activity and favorable ADME-Tox profiles as well as in vivo efficacy. We also describe an approach to mitigate the resulting phototoxic liability in the course of our optimization campaign.

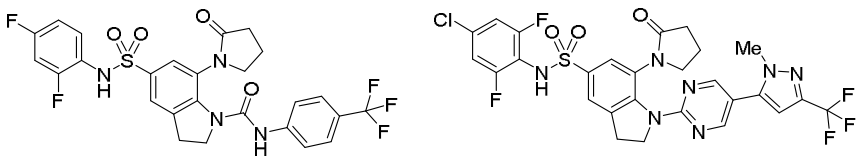

2
hMGAT2 IC_{50} = 3.4 nM

27c
hMGAT2 IC_{50} = 7.8 nM

Figure 1. *N*-Phenylindoline-5-sulfonamide-based MGAT2 inhibitors.

2. Chemistry

Scheme 1 details the synthesis of the *N*-(4-chloro-2,6-difluorophenyl)indoline-5-sulfonamide derivatives **9a** and **9b**. As described in a previous report,[13] the sulfonyl chloride **3** smoothly reacted with 2,4-difluoroaniline or *p*-anisidine in *N*,*N*-dimethylacetamide without the addition of a base to give the corresponding sulfonamide in good yields. However, the reaction of **3** with 4-chloro-2,6-difluoroaniline resulted in a poor yield (10–20% yield) under the same condition, probably because of the low basicity and nucleophilicity of the aniline. After condition screening, we found that this sulfonamidation proceeded cleanly under refluxing in 2,2,2-trifluoroethanol as a solvent, which afforded much better results than conditions using a base such as pyridine, *N*,*N*-diisopropylethylamine, or sodium hydride. The slightly acidic nature of 2,2,2-trifluoroethanol may be involved in the positive effect for this reaction because the use of ethanol or ethyl acetate as a solvent for this type of reaction gave no or little desired product. For substrates with an acid-labile substituent, the addition of molecular sieves 4A was effective in scavenging the generated hydrogen chloride. After the reduction of the nitro group of **4** with zinc powder, the desired aniline **5** was obtained in a good isolated yield. Acylation of **5** with 4-chlorobutyryl chloride followed by intramolecular cyclization using sodium hydride furnished lactam **7**. The benzyloxycarbonyl (Cbz) group of **7** was removed by hydrolysis under a basic condition to give **8**, which was subjected to urea or carbamate formation at the indoline 1-position to provide the final product **9a** or **9b**. The requisite *N*-(2,2,3,3,3-pentafluoropropyl)piperidine **11** was prepared from 4-hydroxypiperidine and 2,2,3,3,3-pentafluoropropyl trifluoromethanesulfonate.

Scheme 1. Synthesis of indoline-5-sulfonamide derivatives **9a** and **9b**[a]

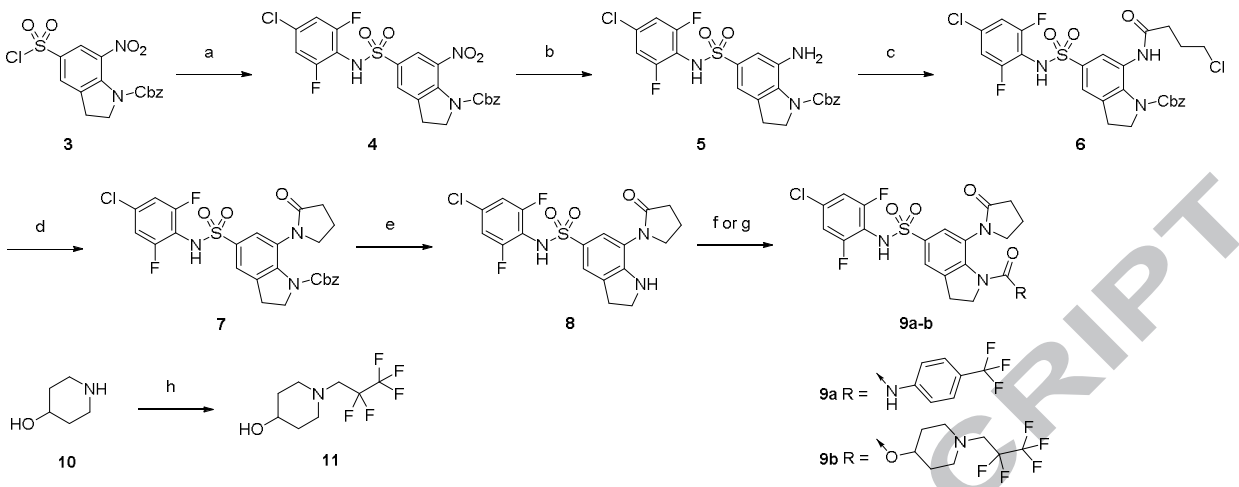

[a]Reagents and conditions: (a) 4-chloro-2,6-difluoroaniline, 2,2,2-trifluoroethanol, MS4A, reflux; (b) Zn, AcOH, rt, 86% over 2 steps; (c) 4-chlorobutyryl chloride, DMA, 0 °C to rt; (d) NaH, DMF, 0 °C to rt, 91% over 2 steps; (e) NaOH, H_2O, THF, MeOH, rt, 87%; (f) 4-(trifluoromethyl)aniline, triphosgene, pyridine, THF, 0 °C; then **8**, TEA, THF, 0 °C to rt, 83%; (g) **11**, triphosgene, TEA, THF, 0 °C to rt; then **8**, THF, 0 °C to rt, 87%; (h) 2,2,3,3,3-pentafluoropropyl trifluoromethanesulfonate, TEA, THF, 0 °C to rt, 88%.

To efficiently access 7-(2-oxopyrrolidin-1-yl)indoline-5-sulfonamide derivatives with various anilines at the 5-position, we employed the method shown in Scheme 2, in which the lactam ring was constructed at the 7-position prior to sulfonamide formation. The nitro group of **12** was selectively reduced with sodium hydrosulfite to give aniline **13**, which was converted to the lactam **15** by a two-step sequence. Palladium-catalyzed coupling of **15** with benzyl mercaptan followed by oxidative chlorination using *N*-chlorosuccinimide (NCS) in aqueous acetic acid gave a common intermediate **17**. After sulfonamidation of **17** with anilines, **18a–c** were transformed to the final products **20a–c** in analogy with compound **9b** in Scheme 1.

Scheme 2. Synthesis of indoline-5-sulfonamide derivatives **20a–c**[a]

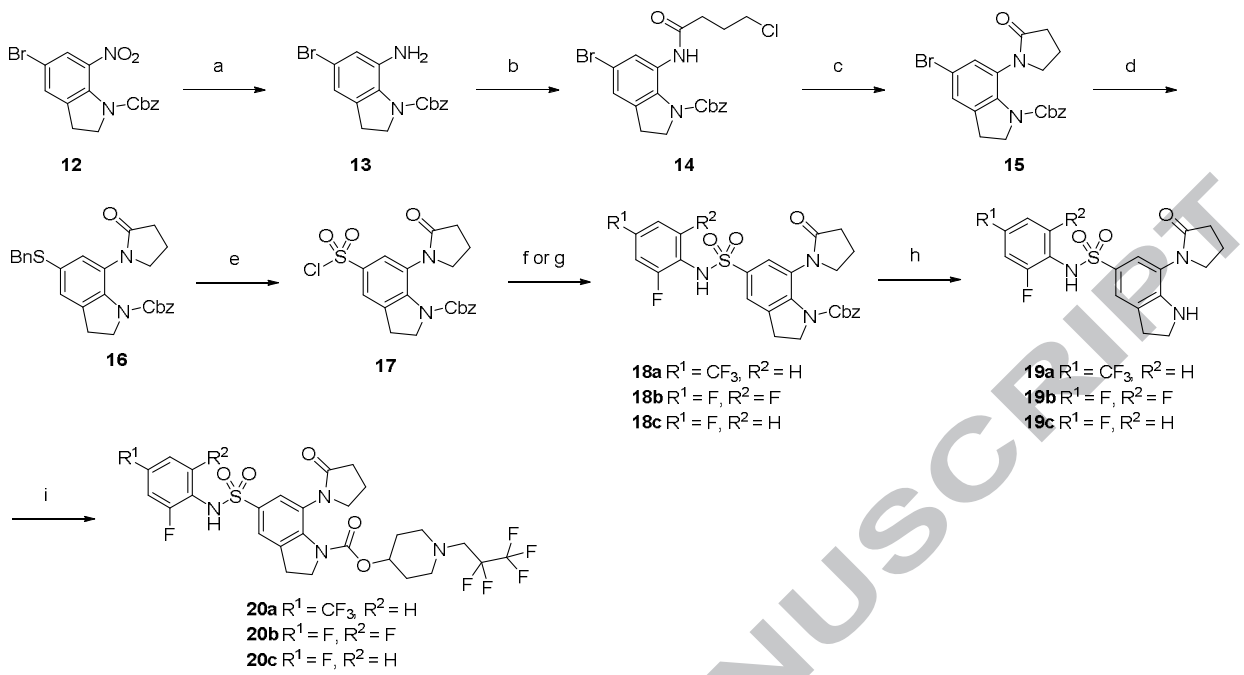

[a]Reagents and conditions: (a) $Na_2S_2O_4$, EtOH, THF, H_2O, 60 °C, 73%; (b) 4-chlorobutyryl chloride, DMA, 0 °C to rt; (c) NaH, DMF, 0 °C to rt, 82% over 2 steps; (d) BnSH, $Pd_2(dba)_3$, Xantphos, DIEA, toluene, reflux, 96%; (e) NCS, AcOH, H_2O, rt, 81%; (f) 2-fluoro-4-(trifluoromethyl)aniline, 2,2,2-trifluoroethanol, 80 °C, 87%; (g) 2,4,6-trifluoroaniline, pyridine, rt, 70%; (h) H_2 (1 atm), Pd on carbon, THF, MeOH, rt, 93%–quant.; (i) **11**, triphosgene, TEA, THF, 0 °C to rt, 59–79%.

Scheme 3 describes the synthetic steps of 1-phenylindoline derivatives. The introduction of a phenyl group at the indoline 1-position of **8** was achieved by Buchwald–Hartwig amination using RuPhos precatalyst, which was reported as an effective catalyst for C–N bond formation between aryl halides and secondary amines,[15, 16] to afford **21** in a moderate yield. Compound **21** underwent a selective bromination upon treatment with one equivalent of *N*-bromosuccinimide (NBS) to give **22**. Finally, Suzuki–Miyaura coupling reaction of **22** with an arylboronic acid provided the desired biphenyl derivative **23**.

Scheme 3. Synthesis of indoline-5-sulfonamide derivative **23**[a]

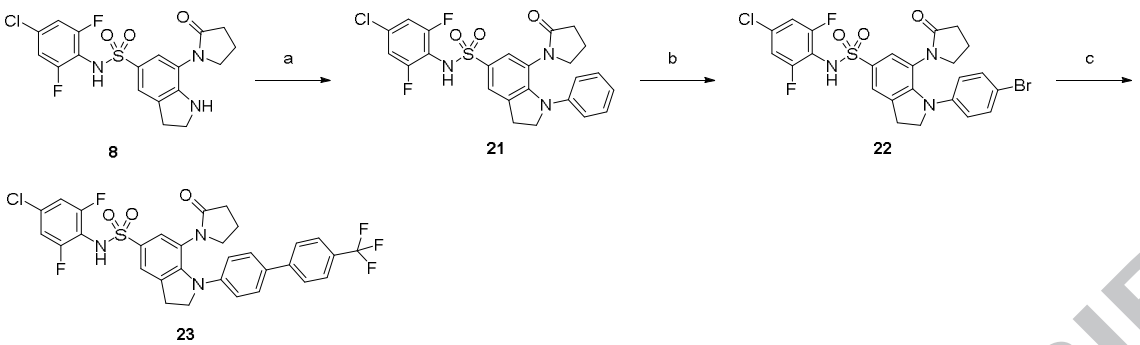

[a]Reagents and conditions: (a) PhBr, RuPhos precatalyst, RuPhos, NaO^{t}Bu, DME, reflux, 65%; (b) NBS, DMF, 0 °C, 99%; (c) 4-(trifluoromethyl)phenylboronic acid, $Pd(PPh_3)_4$, K_2CO_3, THF, reflux, 63%.

1-(Pyrimidin-2-yl)indoline derivatives **27a–f** were synthesized using the methods depicted in Scheme 4. Nucleophilic substitution reaction of **8** with 2-chloro-5-nitropyrimidine cleanly proceeded under refluxing in THF to furnish **24** in a good yield. This type of S_NAr reaction of **8** required an electron-withdrawing group on the pyrimidine ring, such as a nitro or alkoxycarbonyl group, for high conversion to the desired compounds. The nitro group of **24** was reduced by hydrogenation using Adams' catalyst (platinum oxide) to give **25**, which was subsequently subjected to Sandmeyer reaction using *n*-pentyl nitrite and copper(II) bromide to provide 5-bromopyrimidine **26**. The final compounds **27a–c** were obtained by palladium-catalyzed coupling reactions of **26** with aryl boronic acids. In contrast, copper-catalyzed N-arylation of the substituted pyrazoles with **26** provided **27d–f**. The chemical structure of **27e** was confirmed by X-ray crystallographic analysis of a single crystal structure (Figure 2), and the structure of **27f** was determined by nuclear magnetic resonance (NMR) experiments.[17]

Scheme 4. Synthesis of indoline-5-sulfonamide derivatives **27a–f**[a]

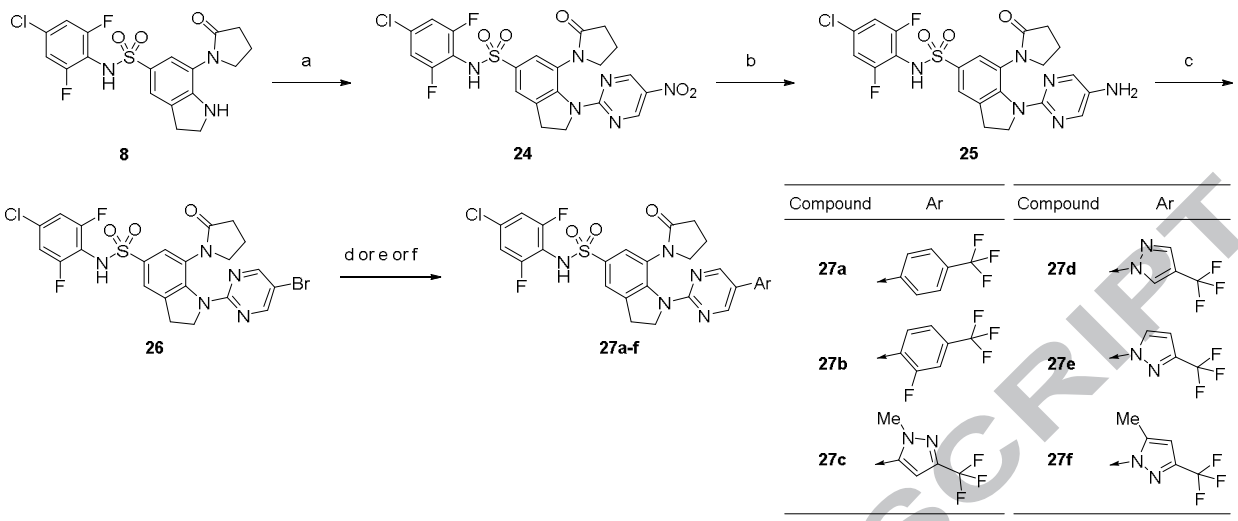

[a]Reagents and conditions: (a) 2-chloro-5-nitropyrimidine, THF, reflux, 98%; (b) H_2 (1 atm), PtO_2, THF, EtOH, rt, 93%; (c) *n*-pentyl nitrite, $CuBr_2$, CH_3CN, 0 °C to 60 °C, 45%; (d) $ArB(OH)_2$, $Pd(PPh_3)_4$, Na_2CO_3, THF/H_2O or DME/H_2O, 110–130 °C (microwave), 50–87% (for **27a** and **27b**); (e) $ArB(OH)_2$, $Pd(PPh_3)_4$, K_2CO_3, THF, reflux, 38% (for **27c**); (f) substituted pyrazole, CuI, 8-quinolinol, K_2CO_3, DMSO, 130°C, 11–42% (for **27d**–**f**).

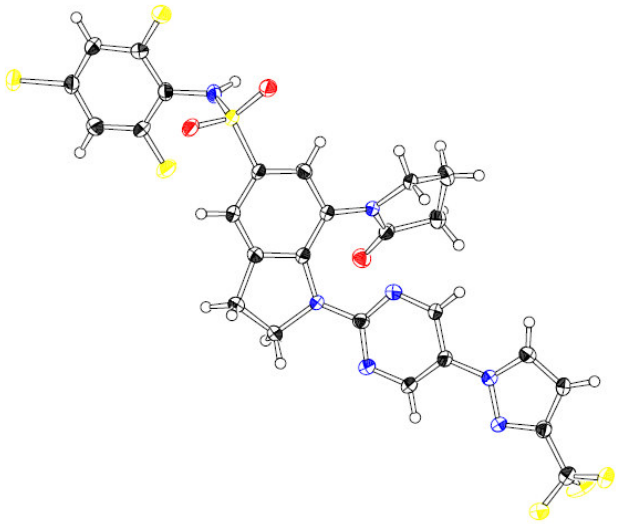

Figure 2. ORTEP of **27e**, thermal ellipsoids are drawn at 50% probability.

Scheme 5 details the synthesis of compounds with a cyclic urea at the indoline 7-position. In

the urea formation reaction of **5** with 2-chloroethyl isocyanate, the addition of a catalytic amount of hydrogen chloride was found to accelerate the reaction rate and suppress undesired urea formation on the sulfonamide nitrogen. The obtained **28** was subsequently subjected to intramolecular cyclization upon treatment with sodium hydride to give cyclic urea **29** in good isolated yields over two steps. Compound **29** was elaborated to the final product **34** in analogy with **27c** in Scheme 4.

Scheme 5. Synthesis of indoline-5-sulfonamide derivative **34**[a]

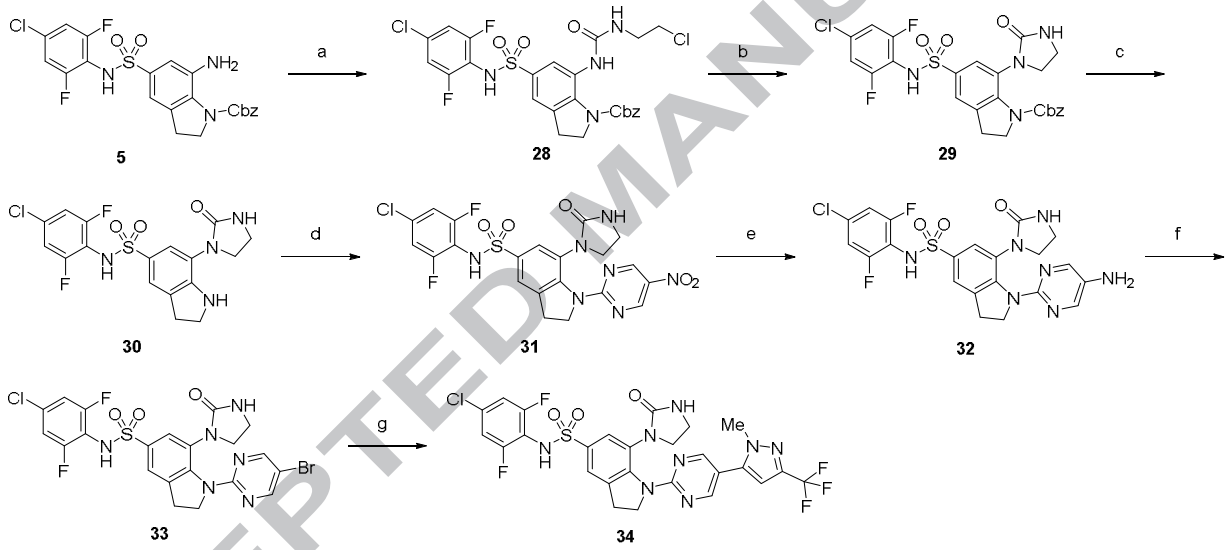

[a]Reagents and conditions: (a) 2-chloroethyl isocyanate, cat. HCl, THF, 70 °C; (b) NaH, DMF, 0 °C to rt, 77% over 2 steps; (c) NaOH, H_2O, THF, MeOH, reflux, 92%; (d) 2-chloro-5-nitropyrimidine, THF, reflux, 92%; (e) H_2 (1 atm), PtO_2, THF, EtOH, rt, 97%; (f) *tert*-butyl nitrite, $CuBr_2$, CH_3CN, rt, 39%; (g) 1-methyl-3-trifluoromethyl-1*H*-pyrazole-5-boronic acid pinacol ester, $Pd(PPh_3)_4$, K_2CO_3, THF, 100 °C (microwave), 46%.

3. Results and Discussion

The newly synthesized compounds were tested for MGAT2 inhibitory activity using membrane fractions from the MGAT2 expression. To obtain in-depth profiles of *N*-

phenylindoline-5-sulfonamide derivatives for the development of novel MGAT2 inhibitors, we conducted further evaluation of compounds **1** and **2** in terms of ADME-Tox profiles. We found that these compounds displayed TDI of CYP3A4, discouraging their further development (Table 1). TDI of CYP3A4 was evaluated by a single-point assay, in which test compounds were preincubated with human liver microsomes in the presence of NADPH before measuring CYP3A4 enzymatic activity toward its specific substrate. Preincubation of compound **1** or **2** with microsomes led to a significant loss of the activity of CYP3A4 relative to that under a condition without preincubation. Another series of indoline-5-sulfonamide-based MGAT2 inhibitors with a non-aromatic ring connected by a carbamate linkage at the 1-position, represented by **20c**, also exhibited possible liability for CYP3A4 TDI. Accordingly, our subsequent optimization effort was directed toward addressing the undesirable CYP3A4 TDI issue of this series of compounds.

Table 1. MGAT2 inhibitory activity and CYP3A4 TDI profiles

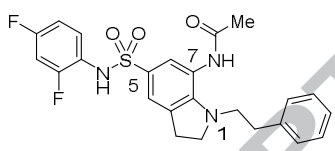

1

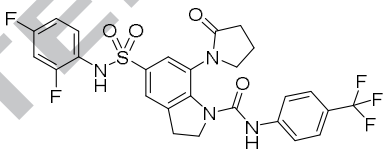

2

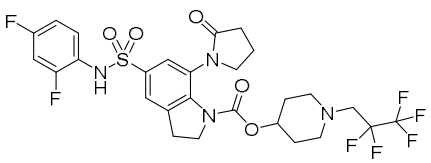

20c

Compound	hMGAT2[a] IC_{50} (nM)	CYP3A4 TDI[b] (% remaining)	$LogD_{7.4}$[c]
1	1.0 (0.89–1.2)	13	2.5
2	3.4 (3.0–3.9)	43	3.1
20c	4.1 (3.4–4.9)	59	3.7

[a] Inhibitory activity against human MGAT2. IC_{50} values are presented as means of duplicate experiments with their 95% confidence intervals in parentheses.
[b] CYP3A4 time dependent inhibition assay (n = 2). The remaining activity of CYP3A4 after preincubation with a test compound was determined.

[c] LogD value at pH 7.4.

We assumed that the 2,4-difluoroaniline moiety, a common structural motif for **1**, **2**, and **20c**, would be the cause of mechanism-based inactivation (MBI) of CYP3A4. Presumed mechanisms of MBI of 2,4-difluoroaniline derivatives are depicted in Figure 3. It has been reported that 4-fluoroanilines are relatively easily subject to CYP-catalyzed defluorination,[18, 19] and this metabolism has the potential to cause bioactivation.[20, 21] We hypothesized that oxidative metabolism of the benzene ring of 2,4-difluoroanilines could generate reactive metabolites such as an epoxide or iminoquinone, which may be attacked by an amino acid residue of the CYP3A4 active site to form a covalent bond, leading to an irreversible inactivation of CYP3A4. According to this hypothesis, structural modifications to the 2,4-difluoroaniline moiety could mitigate TDI liability. Our compound design was based on the following concepts: 1) replacement of the fluorine atom at the 4-position with a substituent more resistant to metabolism and 2) introduction of an electron-withdrawing group onto the benzene ring to lower susceptibility to oxidative metabolism.

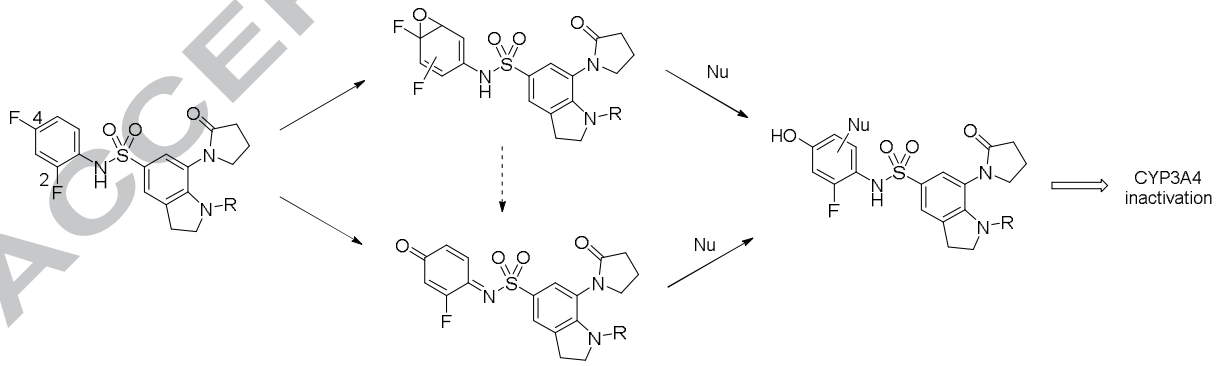

Figure 3. Postulated mechanism of CYP3A4 inactivation

Table 2 summarizes results of CYP3A4 TDI of representative compounds together with their MGAT2 inhibitory activities. Gratifyingly, the conversion of the 4-F group of **20c** to a trifluoromethyl group significantly improved CYP3A4 TDI risk (**20a**). Reducing the electron density of the aniline moiety by introducing an additional fluorine atom also conferred a beneficial effect on CYP3A4 TDI profile, and the 2,4,6-trifluoroaniline derivative **20b** did not inactivate CYP3A4 after preincubation. These results clearly indicated that the 2,4-difluoroaniline moiety of **1**, **2**, or **20c** was the cause of CYP3A4 TDI. Unfortunately, the improvement of CYP3A4 TDI of compounds **20a** and **20b** was accompanied by a 10–20-fold decline in potency in comparison with that of the corresponding 2,4-difluoroaniline derivative **20c**. Further exploration of the aniline ring substitution led to the identification of 4-chloro-2,6-difluoroaniline as a desirable aniline motif for this series of compounds that could eliminate CYP3A4 TDI liability and minimize the decrease in potency as shown by compound **9b**. In terms of ligand lipophilicity efficiency,[22] compound **9b** displayed the highest LLE value among **20a**, **20b**, and **9b**. The impact of 4-chloro-2,6-difluoroaniline on CYP3A4 TDI was also confirmed by the comparison of 1-carbamoylindoline derivatives **9a** and **2**, although a concomitant loss of potency was observed as in the case of the carbamates (**9b** vs **20c**).

Table 2. MGAT2 inhibitory activity and CYP3A4 TDI profiles

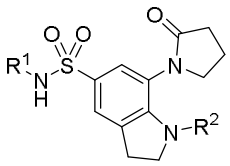

Compound	R^1	R^2	hMGAT2[a] IC_{50} (nM)	CYP3A4 TDI[b] (% remaining)	$LogD_{7.4}$[c]	LLE[d]

20a	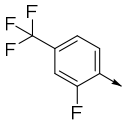	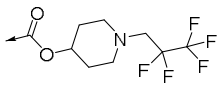	42 (32–55)	93	4.1	3.3
20b	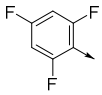	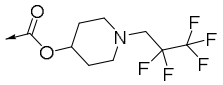	75 (58–96)	95	3.4	3.7
9b	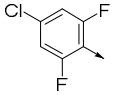	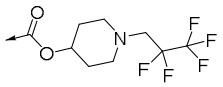	19 (15–24)	82	3.8	3.9
9a	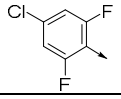	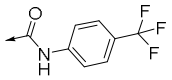	30 (26–34)	89	3.3	4.2

[a] Inhibitory activity against human MGAT2. IC_{50} values are presented as means of duplicate experiments with their 95% confidence intervals in parentheses.
[b] CYP3A4 time dependent inhibition assay (n = 2). The remaining activity of CYP3A4 after preincubation with a test compound was determined.
[c] LogD value at pH 7.4.[23]
[d] LLE = $pIC_{50} - LogD_{7.4}$.

Given the desired aniline moiety with balanced profiles, our subsequent optimization effort was directed to structural modification at the indoline 1-position with the aim of enhancing MGAT2 inhibitory activity. We applied a strategy to rigidify the substituent at the indoline 1-position to restrict conformation of the terminal hydrophobic motif, which is important for interaction with MGAT2.[13] Thereby, several biaryl-type substituents at the 1-position were designed by the conversion of the urea linkage of **9a** to an aryl ring (Figure 4).

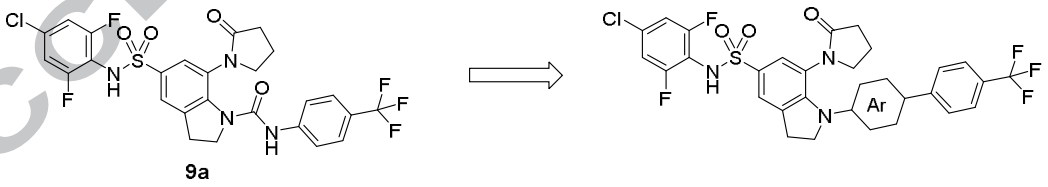

Figure 4. Design stage from 1-carbamoylindoline derivatives to 1-arylindoline derivatives

The MGAT2 activities of the ensuing biaryl derivatives are presented in Table 3. The biphenyl

analog **23** exhibited dramatically enhanced MGAT2 inhibitory activity with an IC_{50} value of 0.25 nM. The LLE value of compound **23** was also considerably improved compared with that of the urea linkage analog **9a**, with a change from 4.2 to 5.1, suggesting that this structural transformation achieved a larger increase in potency than simply expected from the change in lipophilicity. Hence, it is supposed that the introduction of the biaryl alignment at the indoline 1-position enabled the terminal trifluoromethylphenyl ring to adopt the desired orientation for efficient interaction with the presumed hydrophobic site of MGAT2. Furthermore, the 5-phenylpyrimidine derivative **27a**, in which two nitrogen atoms were embedded at the corresponding positions to the hetero atoms of the urea linkage of **9a**, also displayed potent MGAT2 inhibitory activity with a subnanomolar IC_{50} value. This modification substantially lowered lipophilicity and thereby further improved the LLE value to 5.4. It was also confirmed that compounds **23** and **27a** displayed no CYP3A4 TDI liability (data not shown).

Table 3. MGAT2 inhibitory activity and phototoxicity profiles

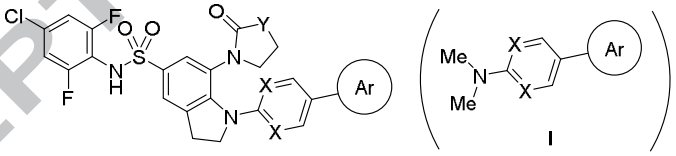

Compound	Ar	X	Y	hMGAT2[a] IC_{50} (nM)	Phototox[b] (% of control)		HOMO–LUMO gap[c] (eV)	$LogD_{7.4}$[d]	LLE[e]
					UV–	UV+			
23	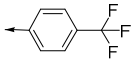	CH	CH_2	0.25 (0.22–0.29)	95 ± 5	2 ± 0	7.90	4.5	5.1
27a	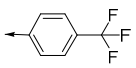	N	CH_2	0.69 (0.59–0.81)	105 ± 8	54 ± 6	8.18	3.8	5.4

27b	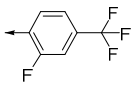	N	CH_2	0.42 (0.37–0.47)	98 ± 6	37 ± 16	8.01	4.1	5.3
27d	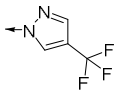	N	CH_2	6.2 (5.5–7.1)	109 ± 7	84 ± 4	8.31	3.1	5.1
27e	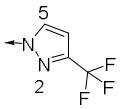	N	CH_2	8.2 (6.7–10)	105 ± 1	91 ± 5	8.31	3.1	5.0
27f	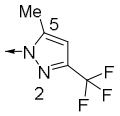	N	CH_2	2.1 (1.9–2.4)	112 ± 4	98 ± 7	8.32	2.9	5.8
27c	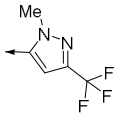	N	CH_2	7.8 (6.6–9.2)	99 ± 8	96 ± 8	8.60	2.8	5.3
34	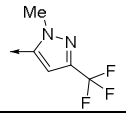	N	NH	3.7 (3.2–4.3)	111 ± 7	107 ± 6	8.60	2.7	5.7

[a] Inhibitory activity against human MGAT2. IC_{50} values are presented as means of duplicate experiments with their 95% confidence intervals in parentheses.
[b] Phototoxicity assay using BALB/c 3T3 cell in the presence of 6.25 μM of compounds. Percentages of control are represented as means ± standard deviation (n = 3).
[c] The HOMO–LUMO energy gap (eV) of each simplified biarylaniline **I** calculated by AM1 method using MOPAC (**23**-**I**, **27a**-**I**, **27b**-**I**, **27d**-**I**, **27e**-**I**, **27f**-**I**, **27c**-**I**, and **34**-**I**).
[d] LogD value at pH 7.4.
[e] LLE = pIC_{50} − $LogD_{7.4}$.

Despite their attractive potencies for MGAT2 inhibition, it was found that the biaryl compounds **23** and **27a** exhibited cytotoxicity against BALB/c 3T3 cells under UV irradiation condition, whereas cytotoxic effect was not observed under a condition without UV exposure (Table 3), thereby indicating potential phototoxic liability. Phototoxicity is one of the drug-induced adverse effects, and it is characterized by an exaggerated inflammatory response to sunlight caused by a photoreactive chemical.[24] Although whether a chemical causes phototoxicity in vivo depends on the distribution of the compound to light-exposed tissues such as the skin or the eyes as well as its photoreactivity, it is necessary to develop a drug candidate that has essentially no potential photoreactivity in terms of patient safety.

We assumed that the biaryl motif at the indoline 1-position of **23** or **27a** would be a chromophore to induce phototoxicity because non-biaryl derivatives such as **9a** did not exert a UV-induced cytotoxic effect (data not shown). To remove the potential phototoxic liability, we implemented a strategy of increasing energy gaps between the highest occupied molecular orbital (HOMO) and the lowest unoccupied molecular orbital (LUMO), focusing on the biaryl motif.[25, 26] A semiempirical molecular orbital method (AM1)[27] using MOPAC was applied in Molecular Operating Environment software (MOE)[28] to calculate the HOMO, LUMO, and HOMO–LUMO energy gaps of biarylanilines **I**, which are simplified versions of each compound (Table 3). According to the calculation, the HOMO orbital of **23**-**I** was localized on the phenyl ring A, whereas the LUMO orbital was mainly found in the phenyl ring B (Figure 5). On the basis of the localization of the HOMO and LUMO orbitals, we reasoned that reduction of the electron density of ring A or enhancement of the electron density of ring B would lead to widening of the HOMO–LUMO energy gap. Indeed, the conversion of phenyl ring A to an electron-deficient pyrimidine ring increased the HOMO–LUMO gap, with a change from 7.90 (**23**-**I**) to 8.18 eV (**27a**-**I**). This transformation improved the phototoxicity risk to some extent, judging from the BALB/c 3T3 cell assay, although compound **27a** still exhibited phototoxic liability. In contrast, the introduction of an electron-withdrawing fluorine atom on the terminal phenyl ring of **27a** to give **27b** reduced the HOMO–LUMO gap and resulted in a similar level of UV-induced cytotoxicity, as displayed by **27a**. These results were in good agreement with our hypothesis based on the relationship between phototoxic potential and the HOMO–LUMO energy gaps of the biaryl moiety.

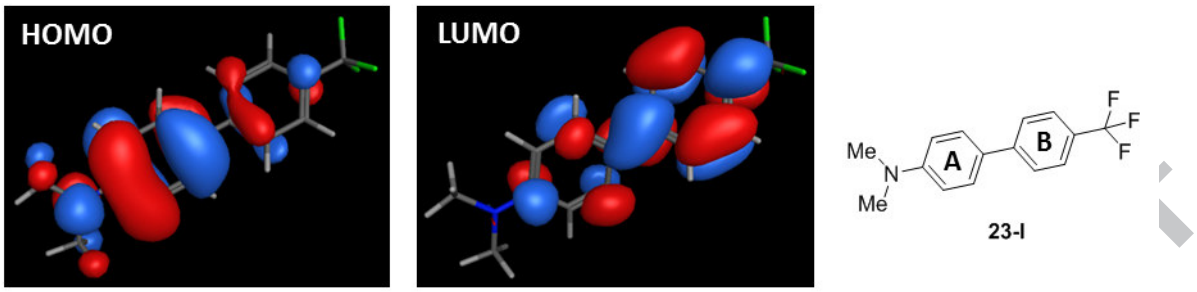

Figure 5. Molecular orbital of HOMO and LUMO of compound **23-I** calculated by MOE (MOPAC, AM1).

We selected 1-(pyrimidin-3-yl)indoline derivatives for further optimization in terms of potent inhibitory activity, lower lipophilicity, and improved phototoxicity liability. The AM1 calculation revealed that the molecular orbital localization of HOMO and LUMO of **27a-I** was similar to that of **23-I**, as shown in Figure 5. To further widen the HOMO–LUMO gap, we designed compounds with an electron-rich 5-membered heterocycle at the 5-position on the pyrimidine ring while maintaining a terminal trifluoromethyl group that could effectively interact with the presumed hydrophobic site of MGAT2.[13] As expected, compared with **27a**, the pyrazole derivatives **27d** and **27e** exhibited larger HOMO–LUMO gaps and greatly improved phototoxic liability (Table 3). These compounds have desirable lipophilicity, with LogD values of approximately 3, and they retained high LLE values of MGAT2 inhibitory activity exceeding 5. Furthermore, the installation of a methyl group at the 5-position on the pyrazole ring of **27e** enhanced MGAT2 inhibitory activity without affecting the phototoxic potential (**27f**). It is worth noting that compound **27f** displayed lower lipophilicity than **27e** (LogD = 2.9 (**27f**) and 3.1 (**27e**)) despite the methyl addition. The calculated LogP value could not predict this change in molecular properties (cLogP = 5.05 (**27f**) and 4.78 (**27e**)). This can be rationalized by the

disruption of an intramolecular hydrogen bond between the pyrazole nitrogen atom at the 2-position and the hydrogen atom on the pyrimidine ring by the methyl addition of **27f**. Because the enhanced potency of **27f** by the methyl addition for MGAT2 inhibition was not likely driven by lipophilicity, it is assumed that the methyl group would have a direct productive interaction with MGAT2.

Following the *N*-linked 1-arylpyrazoles **27d–f**, a *C*-linked 5-arylpyrazole **27c**, in which a beneficial methyl group was introduced on the pyrazole ring, was also investigated. Compound **27c** displayed potent MGAT2 inhibitory activity, with an IC_{50} value of 7.8 nM. In addition, this compound had a widened HOMO–LUMO energy gap and exhibited clearly improved phototoxic liability relative to **27a**. To further enhance MGAT2 inhibitory activity without increasing lipophilicity, the electron density on the carbonyl group at the indoline 7-position was increased by replacement with a cyclic urea motif according to the knowledge we previously reported.[13] This approach was found to be effective in the biaryl series, and the consequent compound **34** exhibited improved potency and reduced lipophilicity, resulting in a higher LLE value. In addition, no phototoxicity was observed for this compound. Taken together, compounds **27f**, **27c**, and **34** demonstrated balanced profiles in terms of MGAT2 inhibitory activity, desirable lipophilicity, and removed phototoxic liability, which made these compounds attractive candidates for further evaluation.

Prior to the in vivo evaluation, the selected compounds **27f**, **27c**, and **34** were evaluated for mouse MGAT2 inhibitory activity, metabolic stability, and pharmacokinetic profiles (Table 4). All three compounds also exhibited potent inhibitory activity against mouse MGAT2, with IC_{50} values of approximately 1 nM and good metabolic stability toward both human and mouse microsomes. The low microsomal clearances of **27f** and **27c** were reflected in low in vivo

clearances in mice (CL_{total} = 471 and 205 mL/h/kg, respectively), and these two compounds displayed favorable pharmacokinetic profiles with good oral bioavailability (F = 52% and 50%, respectively) and prolonged MRTs (2.6 and 3.3 h, respectively) after oral administration at the dose of 1 mg/kg. In sharp contrast to **27c**, the corresponding cyclic urea analog **34** displayed modest oral bioavailability and low plasma concentration despite its low microsomal clearance. Given a comparable aqueous solubility of **34** relative to **27c** (data not shown), this result was likely attributed to the poor membrane permeability of **34** (PAMPA permeability = 166 (**27c**) and 40 (**34**) nm/s). A similar negative impact of the one-atom conversion to cyclic urea on pharmacokinetic profiles was also previously observed in the series of 1-carbamoylindoline derivatives.[13] Consequently, a lactam ring serves as a desirable substituent at the indoline 7-position with a balanced profile of potency, physicochemical profiles, and pharmacokinetic parameters.

Table 4. MGAT2 inhibitory activity, metabolic stability, and pharmacokinetic profiles

Compound	mMGAT2[a] IC_{50} (nM)	CL_{int}[b] (μL/min/mg)		Pharmacokinetic profiles in mice[c, d]					PAMPA[e] (nm/sec)
		HLM	MLM	Vdss[c] (mL/kg)	CL_{total}[c] (mL/h/kg)	AUC[d] (ng·h/mL)	MRT[d] (h)	F[d] (%)	
27f	1.1 (0.82–1.5)	ND	27	1019	471	1120	2.6	52	185
27c	2.4 (2.1–2.7)	ND	ND	539	205	2436	3.3	50	166
34	1.9 (1.6–2.3)	4	33	1964	2368	72	2.3	16	40

[a] Inhibitory activity against mouse MGAT2. IC_{50} values are presented as means of duplicate experiments with their 95% confidence intervals in parentheses.
[b] Human/mouse liver microsomal clearance. ND: The decrease of the compound concentration was not observed.
[c] 0.1 mg/kg, iv.
[d] 1 mg/kg, po.
[e] PAMPA permeability at pH 7.4.

Compound **27c** was selected as a representative compound and evaluated for target selectivity. This compound exhibited IC_{50} values of more than 10 μM against DGAT1, DGAT2, and ACAT1, thereby demonstrating excellent MGAT2 selectivity over related acyltransferases. The potent MGAT2 inhibitory activity, high selectivity over other acyltransferases, and favorable pharmacokinetic profile of **27c** motivated us to evaluate the in vivo efficacy by oral administration.

We conducted OFTT using C57BL/6J mice to examine the compound's effect on hypertriglyceridemia following olive oil challenge. To measure the accumulation of plasma TG, mice were pre-treated with a lipoprotein lipase (LPL) inhibitor, Pluronic F127 (Poloxamer 407), which inhibits the hydrolysis of plasma TG by LPL.[29] Compound **27c** was orally administered 6 h before the oral olive oil challenge, and the plasma chylomicron TG concentration was monitored for 4 h. As shown in Figure 6, the plasma TG excursion was effectively suppressed by the administration of **27c**. The inhibitory effect of **27c** on TG elevation was dose-dependent and significant ($p < 0.025$) at doses of 1 and 3 mg/kg. The inhibition degree of TG by **27c** at the dose of 3 mg/kg was comparable with that observed in MGAT2 gene knockout mice (unpublished data), suggesting that this compound nearly completely inhibited MGAT2 in vivo at this dose. These results promised that compound **27c** would exhibit beneficial pharmacological effects for the treatment of metabolic disorders.

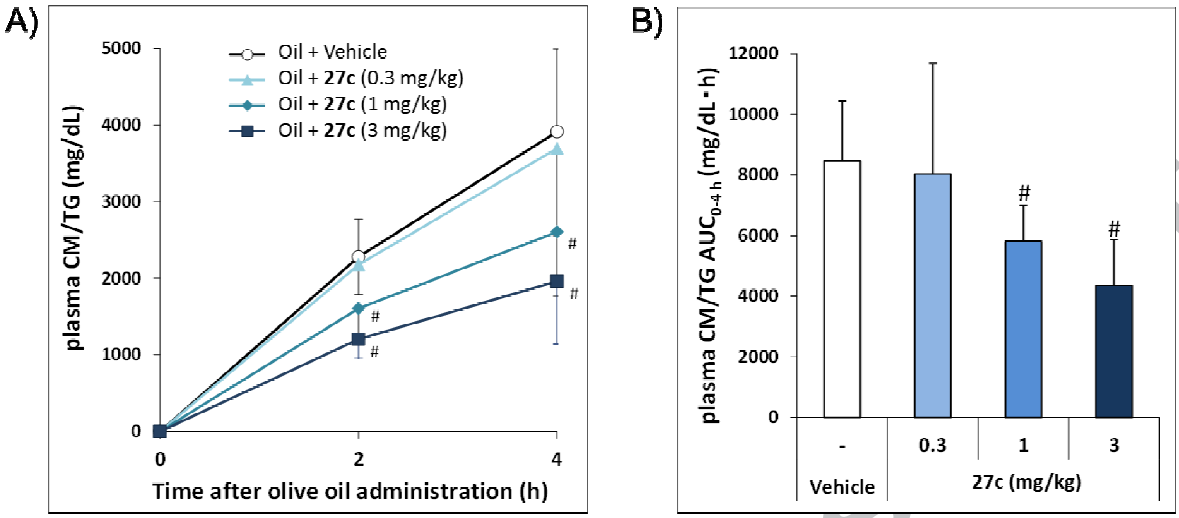

Figure 6. Effect of **27c** on plasma TG elevation during oral fat tolerance test in C57BL/6J mice. **27c** (0.3, 1, 3 mg/kg) was orally administered 6 h prior to olive oil load. (A) Changes in plasma chylomicron/TG (CM/TG) levels after olive oil load. (B) Area under the curve (AUC) of plasma CM/TG levels during 4 h after oil load. Data are the mean ± SD (n = 5). #, $p \leq 0.025$ versus vehicle by William's test.

Compound **27c** was further assessed in terms of the DDI potential. As shown in Table 5, eliminated liability for CYP3A4 TDI of **27c** was confirmed. In addition, this compound exhibited little or no reversible inhibition against major CYP isoforms (1A2/2C8/2C9/2D6/3A4) at the concentration of 10 μM. These results were suggestive of a safe DDI profile of **27c,** and they warrant further development of this compound.

Table 5. CYP3A4 TDI and reversible CYP inhibition profiles of **27c**

Compound	CYP3A4 TDI[a] (% remaining)	Reversible CYPs inhibition (% inhibition at 10 μM)

		1A2	2C8	2C9	2D6	3A4
27c	107	< 10	32	17	< 10	< 10

[a] CYP3A4 time dependent inhibition assay (n = 2). The remaining activity of CYP3A4 after preincubation with a test compound was determined.

4. Conclusion

MGAT2 has emerged as a potential peripheral target for the treatment of obesity and metabolic disorders. To develop a novel class of MGAT2 inhibitors with desirable DMPK and toxicological profiles, we continued our optimization campaign of *N*-phenylindoline-5-sulfonamide derivatives for addressing the potential CYP3A4 TDI liability. Structural modification was focused on the 2,4-difluoroaniline motif on the basis of the hypothesis of oxidative bioactivation of this moiety. Replacement of the fluorine atom at the 4-position with a substituent more resistant to metabolism was combined with the introduction of an additional fluorine atom on the benzene ring to reduce electron density, resulting in the identification of 4-chloro-2,6-difluoroaniline derivatives that lacked CYP3A4 TDI liability, with minimal loss of MGAT2 inhibition potency. Subsequently, biaryl substituents were introduced at the 1-position to enhance MGAT2 inhibitory activity. The resulting phototoxic liability was successfully removed by an appropriate ring alignment based on the HOMO–LUMO gap hypothesis, which led to the discovery of **27c**. Compound **27c** exhibited potent and selective MGAT2 inhibitory activity, desirable physicochemical properties, favorable oral bioavailability, and prolonged pharmacokinetic profiles in mice. These profiles were reflected in the potent in vivo efficacy, and **27c** thereby effectively suppressed plasma TG excursion after olive oil loading in OFTT. Taken together, these results suggest that **27c** could have a therapeutic potential for the treatment of metabolic diseases, including obesity, as observed in MGAT2 gene knockout mice. Further pharmacological evaluation of this compound will be disclosed in due course.

5. Experimental section

5.1. Chemistry

Melting points were determined in open capillary tubes on a Büchi melting point apparatus B545 and are uncorrected. ^{1}H NMR spectra and ^{13}C NMR spectra were recorded on Bruker AVANCE III (300 MHz) or Bruker Advance III plus (400 MHz) spectrometer. Chemical shifts are given in parts per million (ppm) downfield from tetramethysilane (δ) as the internal standard in deuterated solvent and coupling constants (*J*) are in Hertz (Hz). Data are reported as follows: chemical shift, integration, multiplicity (s = singlet, d = doublet, t = triplet, q = quartet, quint = quintet, dd = doublet of doublets, dt = doublet of triplets, dq = doublet of quartets, td = triplet of doublets, tt = triplet of triplets, tq = triplet of quartets, qd = quartet of doublets, qt = quartet of triplets, ddd = doublet of doublet of doublets, m = multiplet, bs = broad signal), and coupling constants. All solvents and reagents were obtained from commercial suppliers and used without further purification. Liquid-liquid extraction in work-up procedures was generally conducted with 30–200 times volume of the indicated organic solvents to the reaction substrates (v/w). Thin-layer chromatography (TLC) was performed on Merck silica gel plates $60F_{254}$. Silica gel column chromatography was performed on Purif-Pack (SI or NH, SHOKO SCIENTIFIC). LC–MS analysis was performed on a Shimadzu Liquid Chromatography–Mass Spectrometer System, operating in APCI (+ or −) or ESI (+ or −) ionization mode. Analytes were eluted using a linear gradient of 0.05% TFA containing water/acetonitrile or 5 mM ammonium acetate containing water/acetonitrile mobile phase. The purities of compounds submitted for biological evaluation were > 95% as determined by elemental analyses within ±0.4% of the calculated values. Yields are not optimized.

5.1.1. Benzyl 7-amino-5-[(4-chloro-2,6-difluorophenyl)sulfamoyl]-2,3-dihydro-1*H*-indole-1-carboxylate (5)

Step A. A mixture of compound **3**[13] (108 g, 271 mmol), 4-chloro-2,6-difluoroaniline (53.2 g, 325 mmol), molecular sieves 4A (pellet, 300 g, unactivated), and 2,2,2-trifluoroethanol (1084 mL) was stirred at reflux for 24 h. After cooling to room temperature, insoluble materials were filtered off through a pad of celite. The filtrate was concentrated under reduced pressure and the residue was diluted with AcOEt–$^{i}Pr_2O$ (1:1 v/v). Insoluble materials were filtered off and the filtrate was concentrated under reduced pressure to give benzyl 5-[(4-chloro-2,6-difluorophenyl)sulfamoyl]-7-nitro-2,3-dihydro-1*H*-indole-1-carboxylate as a brown amorphous solid (**4**, 142 g). This product was used for the next step without further purification. MS (ESI/APCI) *m/z* 522.1 $[M - H]^-$. ^{1}H NMR (300 MHz, DMSO-d_6) δ 3.19–3.29 (2H, m), 4.27 (2H, t, J = 8.4 Hz), 5.20 (2H, s), 7.26–7.53 (7H, m), 7.80–8.06 (2H, m), 10.35 (1H, s).

Step B. To a mixture of compound **4** (142 g) obtained above in acetic acid (1506 mL) was added portionwise zinc powder (89.0 g, 1.36 mol) at room temperature. The mixture was stirred with a mechanical stirrer at room temperature for 13 h under N_2 atmosphere. THF was added to the reaction mixture followed by stirring at room temperature for 1.5 h. Insoluble materials were removed by filtration through a pad of celite and the filter cake was washed with THF. After the filtrate was concentrated under reduced pressure, the residue was suspended in AcOEt and stirred at 70 °C. $^{i}Pr_2O$ was added to the mixture at 70 °C followed by stirring for 10 min at the same temperature. After cooling to room temperature, the precipitated solid was collected, successively washed with AcOEt–$^{i}Pr_2O$ (1:2 v/v) and $^{i}Pr_2O$, and dried under reduced pressure to give the title compound as a pale purple solid (**5**, 116 g, 235 mmol, 86% over 2 steps). MS (ESI/APCI) *m/z* 494.2 $[M + H]^+$. ^{1}H NMR (400 MHz, DMSO-d_6) δ 2.99 (2H, t, J = 8.0 Hz), 4.09

(2H, t, *J* = 8.1 Hz), 5.22 (2H, s), 5.67 (2H, br s), 6.85 (1H, s), 6.96 (1H, s), 7.31–7.57 (7H, m), 9.57–10.03 (1H, m).

5.1.2. Benzyl 5-[(4-chloro-2,6-difluorophenyl)sulfamoyl]-7-(2-oxopyrrolidin-1-yl)-2,3-dihydro-1*H*-indole-1-carboxylate (7)

To a mixture of compound **5** (98.5 g, 199 mmol) in DMA (985 mL) was added 4-chlorobutyryl chloride (33.7 g, 239 mmol) at 0 °C. The mixture was stirred at room temperature overnight. The reaction mixture was quenched with water at 0 °C and extracted with AcOEt. The organic layer was separated, washed with water and brine, dried over $MgSO_4$, and concentrated under reduced pressure. The residue was dissolved in DMF (1 L) and thereto sodium hydride (60% oil dispersion, 17.5 g, 437 mmol) was added at 0 °C. The mixture was stirred at room temperature for 2 h. The reaction was quenched by addition of saturated aqueous NH_4Cl solution at 0 °C and the mixture was extracted with AcOEt. The organic layer was separated, washed with water and brine, dried over $MgSO_4$. After removal of the solvent, the residue was crystallized from AcOEt–$^{i}Pr_2O$ to give the title compound as a light brown crystal (102 g, 182 mmol, 91% over 2 steps). MS (ESI/APCI) *m/z* 562.3 $[M + H]^+$. ^{1}H NMR (400 MHz, DMSO-d_6) δ 1.93–2.06 (2H, m), 2.15–2.25 (2H, m), 3.12 (2H, t, *J* = 7.8 Hz), 3.68 (2H, t, *J* = 6.0 Hz), 4.13 (2H, t, *J* = 7.8 Hz), 5.16 (2H, s), 7.30–7.44 (7H, m), 7.48 (2H, br s), 10.05 (1H, s). ^{13}C NMR (101 MHz, DMSO-d_6) δ 18.2, 27.6, 30.0, 48.9, 49.7, 66.9, 112.7 (t, *J* = 16.9 Hz), 113.1–113.4 (m), 120.3, 124.3, 126.1, 127.5, 127.9, 128.3, 132.7 (t, *J* = 12.8 Hz), 135.4, 136.3, 137.0, 140.1, 151.6, 158.9 (dd, *J* = 253.5, 5.5 Hz), 171.9. Mp 197–199 °C.

5.1.3. *N*-(4-Chloro-2,6-difluorophenyl)-7-(2-oxopyrrolidin-1-yl)-2,3-dihydro-1*H*-indole-5-sulfonamide (8)

A mixture of compound **7** (97.5g, 173 mmol), 8 N aqueous NaOH solution (651 mL), MeOH

(560 mL), and THF (560 mL) was stirred at room temperature for 3 days under N_2 atmosphere. After cooling to 0 °C, the reaction mixture was neutralized with 1 M hydrochloric acid. The mixture was extracted with AcOEt, washed with water and brine, dried over $MgSO_4$, and concentrated under reduced pressure. The residue was crystallized from AcOEt–hexane–$^{i}Pr_2O$ to give the title compound as a light brown solid (64.8 g, 152 mmol, 87%). MS (ESI/APCI) *m/z* 428.1 $[M + H]^+$. ^{1}H NMR (400 MHz, DMSO-d_6) δ 2.02–2.15 (2H, m), 2.38 (2H, t, *J* = 7.8 Hz), 3.03 (2H, t, *J* = 8.5 Hz), 3.51–3.68 (4H, m), 6.07 (1H, br s), 7.16 (1H, s), 7.25 (1H, s), 7.38 (2H, d, *J* = 7.9 Hz), 9.61 (1H, br s). ^{13}C NMR (101 MHz, DMSO-d_6) δ 18.4, 28.4, 30.7, 46.2, 48.4, 113.0–113.3 (m), 118.9, 120.8, 124.2, 126.9, 131.2, 132.3 (t, *J* = 13.2 Hz), 151.0, 159.0 (dd, *J* = 253.8, 5.9 Hz), 173.5. Mp 146–149 °C.

5.1.4. 5-[(4-Chloro-2,6-difluorophenyl)sulfamoyl]-7-(2-oxopyrrolidin-1-yl)-*N*-[4-(trifluoromethyl)phenyl]-2,3-dihydro-1*H*-indole-1-carboxamide (9a)

To a mixture of 4-(trifluoromethyl)aniline (113 mg, 0.701 mmol) and pyridine (0.056 mL, 0.70 mmol) in THF (2 mL) was added triphosgene (72.8 mg, 0.245 mmol) at 0 °C. After stirring at 0 °C for 40 min, the mixture was added to a mixture of compound **8** (150 mg, 0.351 mmol) and triethylamine (0.147 mL, 1.05 mmol) in THF (2 mL) at 0 °C. The resulting mixture was stirred at room temperature overnight. The reaction was quenched by addition of 0.02 M hydrochloric acid and the mixture was extracted with AcOEt. The organic layer was successively washed with aqueous $NaHCO_3$ solution and brine, dried over $MgSO_4$, and concentrated under reduced pressure. The residue was purified by silica gel column chromatography (hexane/AcOEt = 70/30 to 30/70) and crystallized from acetone–$^{i}Pr_2O$ to give the title compound as a white solid (179 mg, 0.292 mmol, 83%). MS (ESI/APCI) *m/z* 615.3 $[M + H]^+$. ^{1}H NMR (300 MHz, DMSO-d_6) δ 1.92–2.06 (2H, m), 2.13–2.24 (2H, m), 3.18 (2H, t, *J* = 8.2 Hz), 3.76 (2H, t, *J* = 6.8 Hz),

4.21 (2H, t, J = 8.3 Hz), 7.36–7.51 (4H, m), 7.60–7.69 (2H, m), 7.70–7.78 (2H, m), 9.56 (1H, s), 10.02 (1H, s). ^{13}C NMR (101 MHz, DMSO-d_6) δ 18.5, 28.0, 30.3, 48.6, 50.8, 112.8 (t, J = 16.9 Hz), 113.1–113.4 (m), 118.7, 120.2, 122.2 (q, J = 31.8 Hz), 124.1, 124.5 (q, J = 271.4 Hz), 125.8, 125.7–125.9 (m), 132.7 (t, J = 13.2 Hz), 134.4, 136.6, 141.2, 143.5, 151.4, 158.9 (dd, J = 253.8, 5.9 Hz), 171.7. Mp 212–214 °C. Anal. Calcd for $C_{26}H_{20}ClF_5N_4O_4S$: C, 50.78; H, 3.28; N, 9.11. Found: C, 50.91; H, 3.20; N, 8.95.

5.1.5. 1-(2,2,3,3,3-Pentafluoropropyl)piperidin-4-yl 5-[(4-chloro-2,6-difluorophenyl)sulfamoyl]-7-(2-oxopyrrolidin-1-yl)-2,3-dihydro-1*H*-indole-1-carboxylate (9b)

To a mixture of 1-(2,2,3,3,3-pentafluoropropyl)piperidin-4-ol (**11**, 98.0 mg, 0.420 mmol) and triethylamine (0.059 mL, 0.42 mmol) in THF (2 mL) was added triphosgene (41.6 mg, 0.140 mmol) at 0 °C. The mixture was stirred at room temperature for 2 h. To the mixture was added dropwise a solution of compound **8** (120 mg, 0.280 mmol) in THF (2 mL) at 0 °C. The resulting mixture was stirred at room temperature overnight. The reaction was quenched by addition of 0.02 M hydrochloric acid and the mixture was extracted with AcOEt. The organic layer was washed with aqueous $NaHCO_3$ solution and brine, dried over $MgSO_4$, and concentrated under reduced pressure. The residue was crystallized from AcOEt–^{i}Pr$_2$O to give the title compound as a white solid (167 mg, 0.243 mmol, 87%). MS (ESI/APCI) *m/z* 687.3 $[M + H]^+$. ^{1}H NMR (300 MHz, DMSO-d_6) δ 1.53–1.74 (2H, m), 1.77–1.94 (2H, m), 2.01–2.17 (2H, m), 2.21–2.38 (2H, m), 2.53–2.66 (2H, m), 2.70–2.86 (2H, m), 3.03–3.29 (4H, m), 3.72 (2H, t, J = 6.9 Hz), 4.02–4.18 (2H, m), 4.64 (1H, dt, J = 7.6, 3.6 Hz), 7.30–7.57 (4H, m), 10.04 (1H, s). ^{13}C NMR (101 MHz, DMSO-d_6) δ 18.3, 27.5, 30.1, 30.2, 49.0, 49.6, 50.7, 55.1 (t, J = 22.4 Hz), 70.3, 112.7 (t, J = 16.9 Hz), 113.1–113.4 (m), 112.0–123.4 (m), 120.3, 124.3, 125.9, 132.7 (t, J = 13.2 Hz), 135.3,

136.9, 140.1, 150.9, 158.9 (dd, J = 253.1, 5.9 Hz), 171.8. Mp 210–212 °C. Anal. Calcd for $C_{27}H_{26}ClF_7N_4O_5S$: C, 47.20; H, 3.81; N, 8.15. Found: C, 47.45; H, 3.75; N, 8.03.

5.1.6. 1-(2,2,3,3,3-Pentafluoropropyl)piperidin-4-ol (11)

Triethylamine (13.8 mL, 98.9 mmol) was added to a mixture of piperidin-4-ol (5.00 g, 49.4 mmol) and 2,2,3,3,3-pentafluoropropyl trifluoromethanesulfonate (16.7 g, 59.3 mmol) in THF (26 mL) at 0 °C. The mixture was stirred at room temperature for 2 days. The reaction was quenched by addition of water and the mixture was extracted with AcOEt. The organic layer was washed with water and brine, dried over Na_2SO_4, and concentrated under reduced pressure to give the title compound as a pale yellow oil (10.1 g, 43.3 mmol, 88%). ^{1}H NMR (300 MHz, DMSO-d_6) δ 1.29–1.45 (2H, m), 1.62–1.74 (2H, m), 2.31–2.42 (2H, m), 2.72–2.84 (2H, m), 3.05–3.20 (2H, m), 3.38–3.51 (1H, m), 4.55 (1H, d, J = 4.2 Hz). ^{13}C NMR (101 MHz, DMSO-d_6) δ 34.2, 51.8, 55.4 (t, J = 22.0 Hz), 65.3, 115.1 (tq, J = 253.1, 35.2 Hz), 118.8 (qt, J = 286.8, 35.9 Hz).

5.1.7. Benzyl 7-amino-5-bromo-2,3-dihydro-1*H*-indole-1-carboxylate (13)

To a mixture of benzyl 5-bromo-7-nitroindoline-1-carboxylate[13] (**12**, 23.2 g, 61.4 mmol) in EtOH (140 mL) and THF (35 mL) was added dropwise a solution of sodium dithionite (42.7 g, 246 mmol) in water (140 mL) at 60 °C. The mixture was stirred at 60 °C overnight. A solution of sodium dithionite (21.4 g, 123 mmol) in water (70 mL) was added to the reaction mixture again at 60 °C and the resulting mixture was stirred at 60 °C overnight. The mixture was diluted with water at 0 °C and extracted with AcOEt. The organic layer was separated, washed with water and brine, dried over $MgSO_4$, and concentrated under reduced pressure. The residue was purified by silica gel column chromatography (hexane/AcOEt = 95/5 to 75/25) to give the title compound as a pale yellow solid (15.5 g, 44.7 mmol, 73%). MS (ESI/APCI) m/z 347.2 $[M + H]^+$. ^{1}H NMR

(400 MHz, DMSO-d_6) δ 2.94 (2H, t, J = 8.0 Hz), 4.02 (2H, t, J = 7.8 Hz), 5.20 (2H, s), 5.55 (2H, br s), 6.66 (1H, s), 6.75 (1H, s), 7.28–7.53 (5H, m).

5.1.8. Benzyl 5-bromo-7-(2-oxopyrrolidin-1-yl)-2,3-dihydro-1*H*-indole-1-carboxylate (15)

Compound **15** was prepared from compound **13** in a manner similar to that described for compound **7** (Purification: silica gel column chromatography (hexane/AcOEt = 90/10 to 50/50)). Pale red solid. Yield 82%. MS (ESI/APCI) *m/z* 415.2 $[M + H]^+$. ^{1}H NMR (400 MHz, DMSO-d_6) δ 1.96 (2H, quint, J = 7.1 Hz), 2.11–2.26 (2H, m), 3.07 (2H, t, J = 7.8 Hz), 3.70 (2H, t, J = 6.8 Hz), 4.06 (2H, t, J = 8.0 Hz), 5.13 (2H, s), 7.25–7.54 (7H, m). ^{13}C NMR (101 MHz, DMSO-d_6) δ 18.2, 28.0, 30.1, 48.7, 49.5, 66.7, 114.9, 125.3, 127.3, 127.5, 127.8, 128.0, 128.3, 135.9, 136.5, 138.4, 151.8, 171.8. Mp 133–135 °C.

5.1.9. Benzyl 5-(benzylsulfanyl)-7-(2-oxopyrrolidin-1-yl)-2,3-dihydro-1*H*-indole-1-carboxylate (16)

A mixture of compound **15** (10.0 g, 24.1 mmol), phenylmethanethiol (3.45 mL, 28.9 mmol), $Pd_2(dba)_3$ (2.21 g, 2.41 mmol), Xantphos (2.79 g, 4.82 mmol), and DIEA (12.6 mL, 72.2 mmol) in toluene (120 mL) was refluxed under N_2 atmosphere overnight. The reaction was quenched by addition of water and the mixture was extracted with AcOEt. The organic layer was separated, washed with water and brine, dried over $MgSO_4$, and concentrated under reduced pressure. The residue was purified by silica gel column chromatography (hexane/AcOEt = 90/10 to 50/50) to give the title compound as a pale yellow solid (10.6 g, 23.1 mmol, 96%). MS (ESI/APCI) *m/z* 459.4 $[M + H]^+$. ^{1}H NMR (400 MHz, DMSO-d_6) δ 1.87–2.04 (2H, m), 2.09–2.25 (2H, m), 3.01 (2H, t, J = 7.8 Hz), 3.67 (2H, t, J = 6.7 Hz), 4.03 (2H, t, J = 7.8 Hz), 4.19 (2H, s), 5.12 (2H, s), 7.03–7.47 (12H, m).

5.1.10. Benzyl 5-(chlorosulfonyl)-7-(2-oxopyrrolidin-1-yl)-2,3-dihydro-1*H*-indole-1-

carboxylate (17)

To a mixture of compound **16** (4.13 g, 9.01 mmol), acetic acid (34 mL), and water (11.3 mL) was added *N*-chlorosuccinimide (4.81 g, 36.0 mmol) at room temperature. The mixture was stirred at room temperature overnight. The reaction mixture was diluted with water and then extracted with AcOEt. The organic layer was separated, washed with water and brine, dried over $MgSO_4$, and concentrated under reduced pressure. The residue was purified by silica gel column chromatography (hexane/AcOEt = 95/50 to 50/50) to give the title compound as a pale yellow amorphous solid (3.16 g, 7.27 mmol, 81%). MS (ESI/APCI) *m/z* 435.3 $[M + H]^+$. ^{1}H NMR (400 MHz, DMSO-d_6) δ 1.91–2.06 (2H, m), 2.11–2.29 (2H, m), 3.04 (2H, t, *J* = 7.8 Hz), 3.69 (2H, t, *J* = 6.9 Hz), 4.06 (2H, t, *J* = 7.9 Hz), 5.14 (2H, s), 7.24–7.46 (7H, m).

5.1.11. Benzyl 5-{[2-fluoro-4-(trifluoromethyl)phenyl]sulfamoyl}-7-(2-oxopyrrolidin-1-yl)-2,3-dihydro-1*H*-indole-1-carboxylate (18a)

A mixture of compound **17** (300 mg, 0.690 mmol) and 2-fluoro-4-(trifluoromethyl)aniline (148 mg, 0.826 mmol) in 2,2,2-trifluoroethanol (3.5 mL) was stirred at 80 °C for 6 h. The reaction mixture was diluted with water and then extracted with AcOEt. The organic layer was separated, washed with water and brine, dried over $MgSO_4$, and concentrated under reduced pressure. The residue was purified by silica gel column chromatography (hexane/AcOEt = 90/10 to 40/60) to give the title compound as a pale yellow amorphous solid (346 mg, 0.599 mmol, 87%). MS (ESI/APCI) *m/z* 578.3 $[M + H]^+$. ^{1}H NMR (400 MHz, DMSO-d_6) δ 1.93–2.06 (2H, m), 2.13–2.28 (2H, m), 3.12 (2H, t, *J* = 8.1 Hz), 3.66 (2H, t, *J* = 6.9 Hz), 4.11 (2H, t, *J* = 8.2 Hz), 5.15 (2H, s), 7.26–7.45 (5H, m), 7.50–7.77 (5H, m), 10.66 (1H, s).

5.1.12. Benzyl 7-(2-oxopyrrolidin-1-yl)-5-[(2,4,6-trifluorophenyl)sulfamoyl]-2,3-dihydro-1*H*-indole-1-carboxylate (18b)

A mixture of compound **17** (700 mg, 1.61 mmol) and 2,4,6-trifluoroaniline (355 mg, 2.41 mmol) in pyridine (4 mL) was stirred at room temperature overnight. The reaction mixture was diluted with water and then extracted with AcOEt. The organic layer was separated, washed with water and brine, dried over $MgSO_4$, and concentrated under reduced pressure. The residue was purified by silica gel column chromatography (hexane/AcOEt = 90/10 to 40/60) to give the title compound as a pale yellow solid (614 mg, 1.13 mmol, 70%). MS (ESI/APCI) *m/z* 546.4 $[M + H]^+$. ^1H NMR (400 MHz, DMSO-d_6) δ 1.91–2.06 (2H, m), 2.14–2.26 (2H, m), 3.12 (2H, t, *J* = 8.0 Hz), 3.68 (2H, t, *J* = 6.8 Hz), 4.13 (2H, t, *J* = 8.2 Hz), 5.16 (2H, s), 7.10–7.60 (9H, m), 9.92 (1H, s). ^{13}C NMR (101 MHz, DMSO-d_6) δ 18.2, 27.6, 30.0, 48.9, 49.7, 66.9, 100.9–101.5 (m), 110.1 (td, *J* = 16.9, 5.1 Hz), 120.4, 124.3, 126.1, 127.5, 127.9, 128.3, 135.4, 136.3, 137.0, 140.0, 151.6, 159.4 (ddd, *J* = 251.6, 16.1, 6.6 Hz), 160.6 (dt, *J* = 248.0, 14.7 Hz), 171.9. Mp 102–104 °C.

5.1.13. *N*-[2-Fluoro-4-(trifluoromethyl)phenyl]-7-(2-oxopyrrolidin-1-yl)-2,3-dihydro-1*H*-indole-5-sulfonamide (19a)

Compound **19a** was prepared from compound **18a** in a manner similar to that described for compound **19c**. Pale red amorphous solid. Yield 93%. MS (ESI/APCI) *m/z* 444.2 $[M + H]^+$. ^1H NMR (400 MHz, DMSO-d_6) δ 2.08 (2H, quint, *J* = 7.4 Hz), 2.38 (2H, t, *J* = 8.0 Hz), 3.02 (2H, t, *J* = 8.8 Hz), 3.50–3.67 (4H, m), 6.15 (1H, s), 7.26–7.70 (5H, m), 10.35 (1H, s).

5.1.14. 7-(2-Oxopyrrolidin-1-yl)-*N*-(2,4,6-trifluorophenyl)-2,3-dihydro-1*H*-indole-5-sulfonamide (19b)

Compound **19b** was prepared from compound **18b** in a manner similar to that described for compound **19c**. Pale yellow amorphous solid. Yield quant. MS (ESI/APCI) *m/z* 412.1 $[M + H]^+$. ^1H NMR (400 MHz, DMSO-d_6) δ 2.08 (2H, quint, *J* = 7.4 Hz), 2.38 (2H, t, *J* = 8.0 Hz), 3.03 (2H,

t, *J* = 8.7 Hz), 3.50–3.69 (4H, m), 6.05 (1H, s), 7.08–7.30 (4H, m), 9.50 (1H, s).

5.1.15. *N*-(2,4-Difluorophenyl)-7-(2-oxopyrrolidin-1-yl)-2,3-dihydro-1*H*-indole-5-sulfonamide (19c)

A mixture of compound **18c**[13] (12.0 g, 22.8 mmol) and 10% palladium on carbon (1.1 g) in a mixed solvent of MeOH (100 mL) and THF (50 mL) was stirred under H_2 atmosphere (1 atm, balloon) at room temperature for 15 h. The catalyst was removed by filtration and the filtrate was concentrated under reduced pressure to give the title compound as a pale yellow amorphous solid (8.90 g, 22.6 mmol, 99%). MS (ESI/APCI) *m/z* 394.1 $[M + H]^+$. ^{1}H NMR (400 MHz, DMSO-d_6) δ 2.07 (2H, quint, *J* = 7.4 Hz), 2.38 (2H, t, *J* = 8.0 Hz), 3.01 (2H, t, *J* = 8.7 Hz), 3.51–3.65 (4H, m), 6.05 (1H, s), 6.94–7.06 (1H, m), 7.12–7.30 (4H, m), 9.67 (1H, s).

5.1.16. 1-(2,2,3,3,3-Pentafluoropropyl)piperidin-4-yl 5-{[2-fluoro-4-(trifluoromethyl)phenyl]sulfamoyl}-7-(2-oxopyrrolidin-1-yl)-2,3-dihydro-1*H*-indole-1-carboxylate (20a)

Compound **20a** was prepared from compound **19a** in a manner similar to that described for compound **9b**. Pale yellow solid. Yield 79%. MS (ESI/APCI) *m/z* 703.4 $[M + H]^+$. ^{1}H NMR (400 MHz, DMSO-d_6) δ 1.51–1.69 (2H, m), 1.77–1.89 (2H, m), 2.07 (2H, quint, *J* = 7.4 Hz), 2.21–2.36 (2H, m), 2.56 (2H, d, *J* = 8.0 Hz), 2.71–2.89 (2H, m), 3.11 (2H, t, *J* = 7.9 Hz), 3.21 (2H, t, *J* = 15.7 Hz), 3.70 (2H, t, *J* = 6.9 Hz), 4.07 (2H, t, *J* = 8.1 Hz), 4.52–4.77 (1H, m), 7.45–7.75 (5H, m), 10.66 (1H, s). ^{13}C NMR (101 MHz, DMSO-d_6) δ 18.3, 27.5, 30.1, 30.2, 48.9, 49.6, 50.7, 55.1 (t, *J* = 22.0 Hz), 70.4, 113.6 (dq, *J* = 22.7, 3.7 Hz), 112.0–123.4 (m), 120.2, 121.8–122.1 (m), 123.2 (qd, *J* = 271.8, 2.6 Hz), 123.9, 124.5, 125.3–126.4 (m), 126.1, 129.1 (d, *J* = 12.5 Hz), 134.3, 137.4, 140.4, 150.9, 153.5 (d, *J* = 248.7 Hz), 171.8. Mp 160–162 °C. Anal. Calcd for $C_{28}H_{27}F_9N_4O_5S$: C, 47.87; H, 3.87; N, 7.97. Found: C, 48.12; H, 3.87; N, 7.86.

5.1.17. 1-(2,2,3,3,3-Pentafluoropropyl)piperidin-4-yl 7-(2-oxopyrrolidin-1-yl)-5-[(2,4,6-trifluorophenyl)sulfamoyl]-2,3-dihydro-1*H*-indole-1-carboxylate (20b)

Compound **20b** was prepared from compound **19b** in a manner similar to that described for compound **9b**. Pale yellow solid. Yield 59%. MS (ESI/APCI) *m/z* 671.4 $[M + H]^+$. ^{1}H NMR (400 MHz, DMSO-d_6) δ 1.55–1.72 (2H, m), 1.85 (2H, dd, *J* = 12.8, 3.8 Hz), 2.07 (2H, quint, *J* = 7.3 Hz), 2.24–2.37 (2H, m), 2.58 (2H, t, *J* = 8.2 Hz), 2.78 (2H, t, *J* = 7.7 Hz), 3.11 (2H, t, *J* = 8.1 Hz), 3.21 (2H, t, *J* = 15.9 Hz), 3.72 (2H, t, *J* = 6.9 Hz), 4.09 (2H, t, *J* = 8.2 Hz), 4.61–4.68 (1H, m), 7.18–7.56 (4H, m), 9.92 (1H, s). ^{13}C NMR (101 MHz, DMSO-d_6) δ 18.3, 27.5, 30.1, 30.2, 49.0, 49.6, 50.7, 55.1 (t, *J* = 22.0 Hz), 70.3, 100.8–101.4 (m), 110.1 (td, *J* = 16.9, 5.1 Hz), 112.0–123.4 (m), 120.3, 124.4, 125.9, 135.3, 136.9, 140.0, 150.9, 159.4 (ddd, *J* = 251.8, 16.0, 6.6 Hz), 160.5 (dt, *J* = 247.4, 15.3 Hz), 171.8. Mp 235–237 °C. Anal. Calcd for $C_{27}H_{26}F_8N_4O_5S$: C, 48.36; H, 3.91; N, 8.36. Found: C, 48.56; H, 3.84; N, 8.29.

5.1.18. 1-(2,2,3,3,3-Pentafluoropropyl)piperidin-4-yl 5-[(2,4-difluorophenyl)sulfamoyl]-7-(2-oxopyrrolidin-1-yl)-2,3-dihydro-1*H*-indole-1-carboxylate (20c)

Compound **20c** was prepared from compound **19c** in a manner similar to that described for compound **9b**. Pale yellow solid. Yield 79%. MS (ESI/APCI) *m/z* 653.4 $[M + H]^+$. ^{1}H NMR (400 MHz, DMSO-d_6) δ 1.56–1.70 (2H, m), 1.79–1.91 (2H, m), 2.01–2.15 (2H, m), 2.24–2.33 (2H, m), 2.57 (2H, t, *J* = 8.1 Hz), 2.71–2.82 (2H, m), 3.09 (2H, t, *J* = 8.1 Hz), 3.20 (2H, t, *J* = 16.1 Hz), 3.69 (2H, t, *J* = 6.9 Hz), 4.07 (2H, t, *J* = 8.2 Hz), 4.63 (1H, tt, *J* = 7.2, 3.7 Hz), 6.95–7.09 (1H, m), 7.21–7.29 (2H, m), 7.41–7.47 (2H, m), 10.03 (1H, s). ^{13}C NMR (101 MHz, DMSO-d_6) δ 18.3, 27.5, 30.1, 30.2, 49.0, 49.6, 50.7, 55.1 (t, *J* = 22.0 Hz), 70.3, 104.6 (dd, *J* = 26.8, 24.6 Hz), 111.6 (dd, *J* = 22.0, 3.7 Hz), 112.0–123.4 (m), 120.3, 120.8 (dd, *J* = 12.8, 4.0 Hz), 124.4, 126.0, 128.5 (dd, *J* = 9.9, 1.8 Hz), 134.7, 137.1, 140.0, 150.9, 156.2 (dd, *J* = 250.5, 12.8 Hz), 159.9 (dd,

J = 245.8, 11.0 Hz), 171.8. Mp 195–197 °C. Anal. Calcd for $C_{27}H_{27}F_7N_4O_5S$: C, 49.69; H, 4.17; N, 8.59. Found: C, 49.81; H, 4.20; N, 8.51.

5.1.19. *N*-(4-Chloro-2,6-difluorophenyl)-7-(2-oxopyrrolidin-1-yl)-1-phenyl-2,3-dihydro-1*H*-indole-5-sulfonamide (21)

A mixture of compound **8** (3.50 g, 8.18 mmol), bromobenzene (1.29 mL, 12.3 mmol), chloro-(2-dicyclohexylphosphino-2′,6′-diisopropoxy-1,1′-biphenyl)[2-(2-aminoethyl)phenyl]palladium(II) methyl *t*ert-butyl ether adduct (RuPhos precatalyst, 1.34 g, 1.64 mmol), dicyclohexyl(2',6'-diisopropoxy-[1,1'-biphenyl]-2-yl)phosphine (RuPhos, 0.763 g, 1.64 mmol), and sodium *tert*-butoxide (2.36 g, 24.5 mmol) in DME (70 mL) was refluxed overnight. The reaction was quenched by addition of 0.1 M hydrochloric acid at 0 °C and the mixture was extracted with AcOEt. The organic layer was separated, washed with water and brine, dried over $MgSO_4$, and concentrated under reduced pressure. The residue was purified by silica gel column chromatography (hexane/AcOEt = 70/30 to 30/70) and crystallized from AcOEt–$^{i}Pr_2O$ to give the title compound as a light brown solid (2.67 g, 5.30 mmol, 65%). MS (ESI/APCI) *m/z* 504.2 $[M + H]^+$. ^{1}H NMR (300 MHz, DMSO-d_6) δ 1.19–1.34 (2H, m), 1.85 (2H, t, *J* = 8.0 Hz), 3.11 (2H, t, *J* = 6.9 Hz), 3.19 (2H, t, *J* = 8.7 Hz), 4.02–4.12 (2H, m), 6.95–7.05 (2H, m), 7.10–7.20 (1H, m), 7.26 (1H, d, *J* = 1.9 Hz), 7.28–7.36 (2H, m), 7.36–7.46 (3H, m), 9.79 (1H, s).

5.1.20. 1-(4-Bromophenyl)-*N*-(4-chloro-2,6-difluorophenyl)-7-(2-oxopyrrolidin-1-yl)-2,3-dihydro-1*H*-indole-5-sulfonamide (22)

To a mixture of compound **21** (2.6 g, 5.16 mmol) in DMF (35 mL) was added *N*-bromosuccinimide (0.964 g, 5.42 mmol) at 0 °C and the mixture was stirred at 0 °C for 1 h. Water was added dropwise to the reaction mixture at 0 °C followed by stirring at room temperature for 1 h. The resulting solid was collected by filtration and washed with EtOH–$^{i}Pr_2O$

(1:3 v/v) to give the title compound as a light brown solid (2.98 g, 5.11 mmol, 99%). MS (ESI/APCI) *m/z* 582.2 $[M + H]^+$. ^{1}H NMR (300 MHz, DMSO-d_6) δ 1.30–1.50 (2H, m), 1.91 (2H, t, *J* = 8.0 Hz), 3.10–3.25 (4H, m), 4.07 (2H, t, *J* = 8.7 Hz), 6.87–6.97 (2H, m), 7.29 (1H, d, *J* = 1.8 Hz), 7.35–7.45 (3H, m), 7.49 (2H, d, *J* = 8.8 Hz), 9.83 (1H, s).

5.1.21. *N*-(4-Chloro-2,6-difluorophenyl)-7-(2-oxopyrrolidin-1-yl)-1-[4'-(trifluoromethyl)biphenyl-4-yl]-2,3-dihydro-1*H*-indole-5-sulfonamide (23)

A mixture of compound **22** (3.67 g, 6.30 mmol), 4-(trifluoromethyl)phenylboronic acid (1.26 g, 6.61 mmol), $Pd(PPh_3)_4$ (0.364 g, 0.315 mmol), and potassium carbonate (6.30 mL, 12.6 mmol) in THF (40 mL) was refluxed for 6 h. The mixture was quenched with 1 M hydrochloric acid and diluted with water and AcOEt. After the organic layer was separated, the aqueous layer was extracted again with a mixed solvent of AcOEt and THF. The combined organic layer was washed with water and brine, dried over $MgSO_4$, and concentrated under reduced pressure. The residue was purified by silica gel column chromatography (hexane/AcOEt = 80/20 to 50/50) and recrystallized from THF–^{i}Pr$_2$O to give the title compound as an off-white solid (2.58 g, 3.98 mmol, 63%). MS (ESI/APCI) *m/z* 648.3 $[M + H]^+$. ^{1}H NMR (300 MHz, DMSO-d_6) δ 1.26–1.43 (2H, m), 1.86–1.99 (2H, m), 3.11–3.28 (4H, m), 4.16 (2H, t, *J* = 8.7 Hz), 7.08 (2H, d, *J* = 8.6 Hz), 7.32 (1H, d, *J* = 1.9 Hz), 7.35–7.46 (3H, m), 7.72 (2H, d, *J* = 8.7 Hz), 7.76–7.84 (2H, m), 7.85–7.95 (2H, m), 9.84 (1H, s). ^{13}C NMR (101 MHz, DMSO-d_6) δ 17.5, 27.4, 29.8, 47.6, 55.7, 113.0 (t, *J* = 16.9 Hz), 113.1–113.4 (m), 120.3, 121.3, 122.1, 124.3 (q, *J* = 271.8 Hz), 125.7 (q, *J* = 3.4 Hz), 126.6, 126.7, 127.0, 127.4 (q, *J* = 32.3 Hz), 130.2, 132.5 (t, *J* = 13.2 Hz), 133.9, 135.0, 143.2, 143.5, 145.2, 159.0 (dd, *J* = 253.5, 5.5 Hz), 172.9. Mp 246–248 °C. Anal. Calcd for $C_{31}H_{23}ClF_5N_3O_3S$: C, 57.45; H, 3.58; N, 6.48. Found: C, 57.53; H, 3.47; N, 6.42.

5.1.22. *N*-(4-Chloro-2,6-difluorophenyl)-1-(5-nitropyrimidin-2-yl)-7-(2-oxopyrrolidin-1-yl)-

2,3-dihydro-1*H*-indole-5-sulfonamide (24)

A mixture of compound **8** (10.0 g, 23.4 mmol) and 2-chloro-5-nitropyrimidine (3.90 g, 24.5 mmol) in THF (80 mL) was refluxed overnight. After removal of the solvent, the residue was purified by silica gel column chromatography (hexane/AcOEt = 70/30 to 0/100) to give the title compound (11.0 g, 20.0 mmol, 98%) as a yellow solid. MS (ESI/APCI) *m/z* 551.2 $[M + H]^+$. ^{1}H NMR (400 MHz, DMSO-d_6) δ 2.07 (4H, br s), 3.22 (2H, t, *J* = 7.8 Hz), 3.94 (2H, br s), 4.45 (2H, t, *J* = 7.7 Hz), 7.44 (2H, d, *J* = 7.7 Hz), 7.56 (1H, s), 7.61 (1H, s), 9.31 (2H, s), 10.13 (1H, s). ^{13}C NMR (101 MHz, DMSO-d_6) δ 18.1, 27.6, 30.1, 48.5, 52.2, 112.6 (t, *J* = 16.9 Hz), 113.1–113.5 (m), 120.1, 123.2, 127.2, 132.8 (t, *J* = 13.2 Hz), 135.6, 136.3, 138.3, 139.1, 154.1, 158.4, 158.9 (dd, *J* = 253.8, 5.9 Hz), 171.1.

5.1.23. 1-(5-Aminopyrimidin-2-yl)-*N*-(4-chloro-2,6-difluorophenyl)-7-(2-oxopyrrolidin-1-yl)-2,3-dihydro-1*H*-indole-5-sulfonamide (25)

A mixture of compound **24** (11.0 g, 20.0 mmol), platinum(IV) oxide (0.907 g), EtOH (444 mL), and THF (222 mL) was stirred under H_2 atmosphere (1 atm, balloon) at room temperature for 3 h. The catalyst was removed by filtration. The filtrate was concentrated under reduced pressure and the residue was crystallized from EtOH–^{i}Pr$_2$O to give the title compound as a white solid (9.64 g, 18.5 mmol, 93%). MS (ESI/APCI) *m/z* 521.2 $[M + H]^+$. ^{1}H NMR (400 MHz, DMSO-d_6) δ 1.79–2.00 (4H, m), 3.12 (2H, t, *J* = 8.3 Hz), 3.62 (2H, t, *J* = 6.1 Hz), 4.19 (2H, t, *J* = 8.5 Hz), 5.08 (2H, br s), 7.34–7.47 (4H, m), 7.98 (2H, s), 9.52 (1H, br s). ^{13}C NMR (101 MHz, DMSO-d_6) δ 17.7, 27.2, 30.2, 48.2, 52.2, 112.8–133.4 (m), 120.3, 123.1, 125.2, 131.3, 132.4 (t, *J* = 13.2 Hz), 135.8, 137.4, 142.4, 143.0, 150.8, 158.9 (dd, *J* = 253.5, 5.5 Hz), 171.2. Mp 164–166 °C.

5.1.24. 1-(5-Bromopyrimidin-2-yl)-*N*-(4-chloro-2,6-difluorophenyl)-7-(2-oxopyrrolidin-1-

yl)-2,3-dihydro-1*H*-indole-5-sulfonamide (26)

To a mixture of compound **25** (9.60 g, 18.4 mmol) in CH_3CN (300 mL) were added *n*-pentyl nitrite (2.50 g, 20.3 mmol) and copper(II) bromide (4.53 g, 20.3 mmol) at 0 °C. The mixture was stirred at room temperature for 1.5 h and then heated at 60 °C for 1 h. The mixture was quenched with 0.02 M hydrochloric acid and extracted with AcOEt. The organic layer was separated, washed with brine, dried over $MgSO_4$, and concentrated under reduced pressure. The residue was purified by silica gel column chromatography (hexane/AcOEt = 70/30 to 0/100) to give the title compound as a yellow solid (4.85 g, 8.29 mmol, 45%). MS (ESI/APCI) *m/z* 584.2 $[M + H]^+$. ^{1}H NMR (400 MHz, DMSO-d_6) δ 1.93–2.11 (4H, m), 3.17 (2H, t, *J* = 8.0 Hz), 3.77–3.87 (2H, m), 4.31 (2H, t, *J* = 8.0 Hz), 7.43 (2H, d, *J* = 7.7 Hz), 7.48 (1H, s), 7.52 (1H, s), 8.71 (2H, s), 10.02 (1H, br s). ^{13}C NMR (101 MHz, DMSO-d_6) δ 17.9, 27.4, 30.3, 48.4, 52.0, 109.3, 112.8 (t, *J* = 16.9 Hz), 113.1–113.4 (m), 120.2, 124.0, 125.5, 132.6 (t, *J* = 13.2 Hz), 134.3, 137.3, 140.6, 156.4, 157.5, 158.9 (dd, *J* = 253.8, 5.9 Hz), 171.0. Mp 229–231 °C.

5.1.25. *N*-(4-Chloro-2,6-difluorophenyl)-7-(2-oxopyrrolidin-1-yl)-1-{5-[4-(trifluoromethyl)phenyl]pyrimidin-2-yl}-2,3-dihydro-1*H*-indole-5-sulfonamide (27a)

A mixture of compound **26** (150 mg, 0.256 mmol), 4-(trifluoromethyl)phenylboronic acid (58.5 mg, 0.308 mmol), $Pd(Ph_3P)_4$ (29.6 mg, 0.0256 mmol), and sodium carbonate (82 mg, 0.77 mmol) in a mixed solvent of THF (1.5 mL) and water (1.5 mL) was stirred at 110 °C for 1 h under microwave irradiation. The mixture was poured into water and extracted with AcOEt. The organic layer was washed with brine, dried over $MgSO_4$, and concentrated under reduced pressure. The residue was crystallized from EtOH–^{i}Pr$_2$O to give the title compound as a white solid (145 mg, 0.223 mmol, 87%). MS (ESI/APCI) *m/z* 650.3 $[M + H]^+$. ^{1}H NMR (400 MHz, DMSO-d_6) δ 1.92–2.11 (4H, m), 3.20 (2H, t, *J* = 8.0 Hz), 3.87 (2H, t, *J* = 6.7 Hz), 4.41 (2H, t, *J*

= 8.2 Hz), 7.44 (2H, d, *J* = 7.3 Hz), 7.48–7.58 (2H, m), 7.85 (2H, d, *J* = 8.3 Hz), 7.99 (2H, d, *J* = 8.2 Hz), 9.01 (2H, s), 10.03 (1H, s). ^{13}C NMR (101 MHz, DMSO-d_6) δ 17.9, 27.5, 30.3, 48.4, 51.8, 112.9 (t, *J* = 18.7 Hz), 113.1–113.4 (m), 120.2, 123.5, 124.1, 124.2 (q, *J* = 271.8 Hz), 125.6, 125.9 (q, *J* = 3.4 Hz), 126.6, 128.0 (q, *J* = 31.5 Hz), 132.6 (t, *J* = 13.2 Hz), 134.1, 137.3, 138.5, 140.9, 155.5, 157.6, 158.9 (dd, *J* = 253.8, 5.1 Hz), 171.0. Mp 274–276 °C. Anal. Calcd for $C_{29}H_{21}ClF_5N_5O_3S$: C, 53.58; H, 3.26; N, 10.77. Found: C, 53.51; H, 3.25; N, 10.67.

5.1.26. *N*-(4-Chloro-2,6-difluorophenyl)-1-{5-[2-fluoro-4-(trifluoromethyl)phenyl]pyrimidin-2-yl}-7-(2-oxopyrrolidin-1-yl)-2,3-dihydro-1*H*-indole-5-sulfonamide (27b)

A mixture of compound **26** (100 mg, 0.171 mmol), 2-fluoro-4-(trifluoromethyl)phenylboronic acid (42.7 mg, 0.205 mmol), $Pd(Ph_3P)_4$ (19.8 mg, 0.0171 mmol), and sodium carbonate (54.4 mg, 0.513 mmol) in a mixed solvent of THF (0.66 mL) and water (0.22 mL) was stirred at 130 °C for 1 h under microwave irradiation. The reaction was quenched with water and the mixture was filtered through a pad of Celite. The filtrate was extracted AcOEt. The organic layer was washed with water and brine, dried over $MgSO_4$, and concentrated under reduced pressure. The residue was purified by silica gel column chromatography (hexane/AcOEt = 80/20 to 30/70) to give the title compound as a pale yellow solid (56.8 mg, 0.0850 mmol, 50%). MS (ESI/APCI) *m/z* 666.1 $[M - H]^-$. ^{1}H NMR (400 MHz, DMSO-d_6) δ 1.90–2.21 (4H, m), 3.07–3.26 (2H, m), 3.77–3.97 (2H, m), 4.32–4.50 (2H, m), 7.35–7.61 (4H, m), 7.73 (1H, d, *J* = 8.0 Hz), 7.83–8.00 (2H, m), 8.85 (2H, br s), 10.04 (1H, br s). ^{13}C NMR (101 MHz, DMSO-d_6) δ 17.8, 27.5, 30.2, 48.4, 51.8, 112.9 (t, *J* = 16.9 Hz), 113.1–113.4 (m), 113.4–113.8 (m), 119.0, 120.2, 121.8–122.0 (m), 123.3 (qd, *J* = 272.2, 2.2 Hz), 124.0, 125.7, 126.9 (d, *J* = 13.9 Hz), 130.0 (qd, *J* = 32.3, 8.8 Hz), 131.2 (d, *J* = 3.7 Hz), 132.6 (t, *J* = 12.8 Hz), 134.3, 137.4, 140.7, 156.9 (d, *J* = 4.4 Hz), 157.4, 158.9 (d,

J = 248.7 Hz), 158.9 (dd, *J* = 253.5, 5.5 Hz), 171.0. Mp 273–275 °C. Anal. Calcd for $C_{29}H_{20}ClF_6N_5O_3S \cdot 0.2AcOEt$: C, 52.20; H, 3.18; N, 10.21. Found: C, 52.46; H, 3.20; N, 9.93.

5.1.27. *N*-(4-Chloro-2,6-difluorophenyl)-1-{5-[1-methyl-3-(trifluoromethyl)-1*H*-pyrazol-5-yl]pyrimidin-2-yl}-7-(2-oxopyrrolidin-1-yl)-2,3-dihydro-1*H*-indole-5-sulfonamide (27c)

Compound **27c** was prepared from compound **26** and 1-methyl-3-trifluoromethyl-1*H*-pyrazole-5-boronic acid in a manner similar to that described for compound **23** (Purification: silica gel column chromatography (hexane/AcOEt = 60/40 to 0/100), crystallization from AcOEt–$^{i}Pr_2O$, and recrystallization from EtOH–heptane). White solid. Yield 38%. MS (ESI/APCI) *m/z* 654.3 $[M + H]^+$. ^{1}H NMR (300 MHz, DMSO-d_6) δ 1.95–2.11 (4H, m), 3.20 (2H, t, *J* = 8.1 Hz), 3.86 (2H, br s), 3.97 (3H, s), 4.40 (2H, t, *J* = 8.1 Hz), 7.06 (1H, d, *J* = 0.5 Hz), 7.38–7.48 (2H, m), 7.49–7.58 (2H, m), 8.82 (2H, s), 10.03 (1H, s). ^{13}C NMR (101 MHz, DMSO-d_6) δ 17.9, 27.5, 30.2, 38.2, 48.4, 51.8, 104.9 (d, *J* = 2.2 Hz), 112.8 (t, *J* = 16.9 Hz), 113.1–113.4 (m), 114.7, 120.2, 121.4 (q, *J* = 268.5 Hz), 124.0, 125.9, 132.6 (t, *J* = 13.2 Hz), 134.5, 137.5, 139.5, 139.6 (q, *J* = 37.9 Hz), 140.6, 156.9, 157.5, 158.9 (dd, *J* = 253.5, 5.5 Hz), 171.1. Mp 149–151 °C. Anal. Calcd for $C_{27}H_{21}ClF_5N_7O_3S$: C, 49.58; H, 3.24; Cl, 5.42; F, 14.52; N, 14.99; S, 4.90. Found: C, 49.76; H, 3.42; Cl, 5.39; F, 14.49; N, 14.56; S, 4.94.

5.1.28. *N*-(4-Chloro-2,6-difluorophenyl)-7-(2-oxopyrrolidin-1-yl)-1-{5-[4-(trifluoromethyl)-1*H*-pyrazol-1-yl]pyrimidin-2-yl}-2,3-dihydro-1*H*-indole-5-sulfonamide (27d)

A mixture of compound **26** (200 mg, 0.342 mmol), 4-(trifluoromethyl)-1*H*-pyrazole (93 mg, 0.68 mmol), copper(I) iodide (13 mg, 0.068 mmol), 8-hydroxyquinoline (20 mg, 0.14 mmol), and potassium carbonate (95 mg, 0.68 mmol) in DMSO (2 mL) was stirred at 130 °C under N_2 atmosphere overnight. The mixture was quenched with saturated aqueous NH_4Cl solution and the insoluble materials were removed by filtration. The filtrate was extracted with AcOEt. The

organic layer was successively washed with water and brine, dried over $MgSO_4$, and concentrated under reduced pressure. The residue was purified by silica gel column chromatography (hexane/AcOEt = 70/30 to 30/70) and crystallized from AcOEt–$^{i}Pr_2O$ to give the title compound as a pale yellow solid (80 mg, 0.13 mmol, 37%). MS (ESI/APCI) *m/z* 640.3 $[M + H]^+$. ^{1}H NMR (300 MHz, DMSO-d_6) δ 1.96–2.10 (4H, m), 3.20 (2H, t, *J* = 8.2 Hz), 3.83 (2H, br s), 4.40 (2H, t, *J* = 8.1 Hz), 7.38–7.47 (2H, m), 7.48–7.57 (2H, m), 8.28 (1H, s), 9.05 (2H, s), 9.18 (1H, s), 10.02 (1H, s). ^{13}C NMR (101 MHz, DMSO-d_6) δ 18.0, 27.5, 30.3, 48.4, 52.0, 112.8 (t, *J* = 16.9 Hz), 113.1–113.4 (m), 113.8 (q, *J* = 37.4 Hz), 120.2, 122.7 (q, *J* = 266.3 Hz), 124.1, 125.6, 127.5, 128.9 (q, *J* = 3.7 Hz), 132.6 (t, *J* = 13.2 Hz), 134.3, 137.3, 138.5–138.6 (m), 140.7, 149.2, 156.7, 158.9 (dd, *J* = 253.5, 5.5 Hz), 171.1. Mp 242–245 °C. Anal. Calcd for $C_{26}H_{19}ClF_5N_7O_3S$: C, 48.79; H, 2.99; N, 15.32. Found: C, 48.82; H, 2.92; N, 15.06.

5.1.29. *N*-(4-Chloro-2,6-difluorophenyl)-7-(2-oxopyrrolidin-1-yl)-1-{5-[3-(trifluoromethyl)-1*H*-pyrazol-1-yl]pyrimidin-2-yl}-2,3-dihydro-1*H*-indole-5-sulfonamide (27e)

Compound **27e** was prepared from compound **26** and 3-(trifluoromethyl)pyrazole in a manner similar to that described for compound **27d** (Purification: silica gel column chromatography (hexane/AcOEt = 60/40 to 10/90) and crystallization from AcOEt–$^{i}Pr_2O$). Yellow solid. Yield 42%. MS (ESI/APCI) *m/z* 640.3 $[M + H]^+$. ^{1}H NMR (300 MHz, DMSO-d_6) δ 1.99–2.09 (4H, m), 3.20 (2H, t, *J* = 8.0 Hz), 3.84 (2H, br s), 4.40 (2H, t, *J* = 8.2 Hz), 7.08–7.13 (1H, m), 7.39–7.47 (2H, m), 7.51 (1H, d, *J* = 1.5 Hz), 7.55 (1H, d, *J* = 1.9 Hz), 8.70 (1H, dd, *J* = 2.6, 1.0 Hz), 9.04 (2H, s), 10.02 (1H, s). ^{13}C NMR (101 MHz, DMSO-d_6) δ 18.0, 27.5, 30.3, 48.4, 52.0, 106.4 (d, *J* = 1.5 Hz), 112.8 (t, *J* = 16.5 Hz), 113.1–113.4 (m), 120.2, 121.2 (q, *J* = 269.0 Hz), 124.0, 125.7, 127.5, 131.3, 132.6 (t, *J* = 12.8 Hz), 134.3, 137.4, 140.7, 142.7 (q, *J* = 37.7 Hz), 149.4, 156.8, 158.9 (dd, *J* = 253.5, 5.5 Hz), 171.1. Mp 175–177 °C. Anal. Calcd for $C_{26}H_{19}ClF_5N_7O_3S$: C,

48.79; H, 2.99; N, 15.32. Found: C, 48.61; H, 2.96; N, 15.01.

5.1.30. *N*-(4-Chloro-2,6-difluorophenyl)-1-{5-[5-methyl-3-(trifluoromethyl)-1*H*-pyrazol-1-yl]pyrimidin-2-yl}-7-(2-oxopyrrolidin-1-yl)-2,3-dihydro-1*H*-indole-5-sulfonamide (27f)

Compound **27f** was prepared from compound **26** and 3-methyl-5-(trifluoromethyl)pyrazole in a manner similar to that described for compound **27d** (Purification: silica gel column chromatography (hexane/AcOEt = 80/20 to 40/60) and crystallization from acetone–$^{i}Pr_2O$). White solid. Yield 11%. MS (ESI/APCI) *m/z* 654.2 $[M + H]^+$. ^{1}H NMR (300 MHz, DMSO-d_6) δ 2.04 (4H, br s), 2.35 (3H, s), 3.21 (2H, t, *J* = 7.9 Hz), 3.87 (2H, br s), 4.41 (2H, t, *J* = 8.1 Hz), 6.82 (1H, s), 7.43 (2H, d, *J* = 7.4 Hz), 7.52 (1H, s), 7.55 (1H, s), 8.83 (2H, s), 10.04 (1H, s). ^{13}C NMR (101 MHz, DMSO-d_6) δ 11.3, 17.9, 27.5, 30.2, 48.4, 52.0, 105.0, 112.8 (t, *J* = 16.9 Hz), 113.1–113.4 (m), 120.2, 121.4 (q, *J* = 268.5 Hz), 123.9, 125.9, 126.5, 132.7 (t, *J* = 12.8 Hz), 134.6, 137.5, 140.5, 141.7 (q, *J* = 37.4 Hz), 142.8, 154.1, 157.1, 158.9 (dd, *J* = 253.5, 5.5 Hz), 171.0. Mp 137–139 °C. Anal. Calcd for $C_{27}H_{21}ClF_5N_7O_3S$: C, 49.58; H, 3.24; N, 14.99. Found: C, 49.56; H, 3.20; N, 14.83.

5.1.31. Benzyl 5-[(4-chloro-2,6-difluorophenyl)sulfamoyl]-7-(2-oxoimidazolidin-1-yl)-2,3-dihydro-1*H*-indole-1-carboxylate (29)

A mixture of compound **5** (10.0 g, 20.3 mmol), 2-chloroethyl isocyanate (2.08 mL, 24.3 mmol), 4 M HCl in AcOEt (0.506 mL, 2.02 mmol), and THF (100 mL) was stirred at 70 °C for 8 h. The reaction mixture was diluted with AcOEt, successively washed with water, saturated aqueous $NaHCO_3$ solution and brine, and dried over Na_2SO_4. The solvent was removed by evaporation to give a pale yellow amorphous solid. To a mixture of the solid obtained above in DMF (120 mL) was added sodium hydride (60% oil dispersion, 1.62 g, 40.4 mmol) at 0 °C. After stirring for 15 min, the reaction mixture was allowed to warm to room temperature

followed by stirring for 2 h. The reaction mixture was cooled to 0 °C again and quenched by addition of water. The resulting mixture was acidified with 1 M hydrochloric acid and extracted with a mixed solvent of AcOEt and THF. The organic layer was successively washed with water and brine, and dried over Na_2SO_4. After removal of the solvent, the residue was suspended in AcOEt–$^{i}Pr_2O$ (ca. 1:1 v/v). The precipitated solid was collected and washed with $^{i}Pr_2O$ to give the title compound as a white solid (8.80 g, 15.6 mmol, 77% over 2 steps). MS (ESI/APCI) *m/z* 563.3 $[M + H]^+$. ^{1}H NMR (300 MHz, DMSO-d_6) δ 3.08 (2H, t, *J* = 7.9 Hz), 3.23–3.31 (2H, m), 3.61–3.71 (2H, m), 4.10 (2H, t, *J* = 8.2 Hz), 5.16 (2H, s), 6.58 (1H, s), 7.30–7.45 (8H, m), 7.52 (1H, d, *J* = 1.8 Hz), 10.02 (1H, s). ^{13}C NMR (101 MHz, DMSO-d_6) δ 27.9, 37.6, 45.2, 49.8, 67.0, 112.8 (t, *J* = 16.9 Hz), 113.1–113.4 (m), 118.8, 123.5, 127.7, 127.8, 127.9, 128.4, 132.6 (t, *J* = 13.2 Hz), 135.7, 136.3, 137.1, 139.2, 152.1, 158.9 (dd, *J* = 253.5, 5.5 Hz), 158.2. Mp 182–183 °C.

5.1.32. *N*-(4-Chloro-2,6-difluorophenyl)-7-(2-oxoimidazolidin-1-yl)-2,3-dihydro-1*H*-indole-5-sulfonamide (30)

A mixture of compound **29** (8.80 g, 15.6 mmol), 4 M aqueous NaOH solution (39.1 mL, 156 mmol), THF (39 mL), and MeOH (39 mL) was stirred at reflux for 5 h. The reaction mixture was neutralized with diluted hydrochloric acid. The precipitated solid was collected, washed with water, and dried to give the title compound as a beige solid (6.20 g, 14.5 mmol, 92%). MS (ESI/APCI) *m/z* 429.1 $[M + H]^+$. ^{1}H NMR (400 MHz, DMSO-d_6) δ 2.94–3.10 (2H, m), 3.40 (2H, t, *J* = 7.8 Hz), 3.51–3.76 (4H, m), 6.12 (1H, s), 6.88 (1H, s), 7.13–7.21 (2H, m), 7.33–7.44 (2H, m), 9.51–9.75 (1H, m). ^{13}C NMR (101 MHz, DMSO-d_6) δ 28.6, 37.8, 45.7, 46.3, 113.0–113.4 (m), 119.6, 120.8, 121.8, 127.3, 130.8, 132.3 (t, *J* = 12.8 Hz), 150.7, 158.9 (dd, *J* = 253.8, 5.9 Hz), 159.5. Mp 195–198 °C.

5.1.33. *N*-(4-Chloro-2,6-difluorophenyl)-1-(5-nitropyrimidin-2-yl)-7-(2-oxoimidazolidin-1-yl)-2,3-dihydro-1*H*-indole-5-sulfonamide (31)

Compound **31** was prepared from compound **30** in a manner similar to that described for compound **24** (Purification: crystallization from THF–$^{i}Pr_2O$). Yellow solid. Yield 92%. MS (ESI/APCI) *m/z* 552.3 $[M + H]^+$. ^{1}H NMR (400 MHz, DMSO-d_6) δ 3.20 (2H, t, *J* = 7.6 Hz), 3.38–3.47 (2H, m), 3.99 (2H, t, *J* = 8.0 Hz), 4.42 (2H, t, *J* = 7.7 Hz), 6.37 (1H, br s), 7.37–7.49 (3H, m), 7.55 (1H, s), 9.31 (2H, s), 10.10 (1H, s). ^{13}C NMR (101 MHz, DMSO-d_6) δ 27.8, 37.6, 45.5, 51.9, 112.7 (t, *J* = 16.9 Hz), 113.1–113.5 (m), 118.8, 122.8, 128.2, 132.7 (t, *J* = 13.2 Hz), 135.3, 136.4, 138.2, 138.3, 154.0, 157.4, 158.6, 158.9 (dd, *J* = 253.8, 5.9 Hz). Mp 265–268 °C.

5.1.34. 1-(5-Aminopyrimidin-2-yl)-*N*-(4-chloro-2,6-difluorophenyl)-7-(2-oxoimidazolidin-1-yl)-2,3-dihydro-1*H*-indole-5-sulfonamide (32)

Compound **32** was prepared from compound **31** in a manner similar to that described for compound **25** (Purification: crystallization from AcOEt–$^{i}Pr_2O$). Gray solid. Yield 97%. MS (ESI/APCI) *m/z* 522.3 $[M + H]^+$. ^{1}H NMR (400 MHz, DMSO-d_6) δ 3.05–3.16 (4H, m), 3.51–3.72 (2H, m), 4.18 (2H, t, *J* = 8.5 Hz), 5.04 (2H, br s), 6.28 (1H, s), 7.26–7.48 (4H, m), 7.96 (2H, s), 9.35–9.95 (1H, m). ^{13}C NMR (101 MHz, DMSO-d_6) δ 27.5, 37.5, 45.0, 52.2, 113.0–113.4 (m), 119.2, 124.8, 125.1, 131.7, 132.3 (t, *J* = 12.8 Hz), 135.6, 137.2, 142.6, 143.2, 151.4, 158.2, 158.9 (dd, *J* = 253.8, 5.9 Hz). Mp 167–169 °C.

5.1.35. 1-(5-Bromopyrimidin-2-yl)-*N*-(4-chloro-2,6-difluorophenyl)-7-(2-oxoimidazolidin-1-yl)-2,3-dihydro-1*H*-indole-5-sulfonamide (33)

To a mixture of copper(II) bromide (51.4 mg, 0.230 mmol) and *tert*-butyl nitrite (0.025 mL, 0.21 mmol) in CH_3CN (2 mL) was added compound **32** (100 mg, 0.192 mmol) at room temperature and the mixture was stirred at room temperature overnight. The mixture was

quenched with 0.02 M hydrochloric acid and diluted with AcOEt–THF. The insoluble materials were removed by filtration and the filtrate was extracted with a mixed solvent of AcOEt and THF. The organic layer was separated, washed with brine, dried over $MgSO_4$, and concentrated under reduced pressure. The residue was purified by silica gel column chromatography (hexane/AcOEt = 50/50 to 10/90) to give the title compound as a light brown amorphous solid (43.7 mg, 0.0746 mmol, 39%). MS (ESI/APCI) *m/z* 585.2 $[M + H]^+$. ^1H NMR (300 MHz, DMSO-d_6) δ 3.15 (2H, t, *J* = 8.0 Hz), 3.26–3.37 (2H, m), 3.78–3.93 (2H, m), 4.29 (2H, t, *J* = 8.1 Hz), 6.34 (1H, s), 7.35–7.46 (3H, m), 7.49 (1H, d, *J* = 1.7 Hz), 8.66 (2H, s), 9.99 (1H, s).

5.1.36. *N*-(4-Chloro-2,6-difluorophenyl)-1-{5-[1-methyl-3-(trifluoromethyl)-1*H*-pyrazol-5-yl]pyrimidin-2-yl}-7-(2-oxoimidazolidin-1-yl)-2,3-dihydro-1*H*-indole-5-sulfonamide (34)

A mixture of compound **33** (43.0 mg, 0.0734 mmol), 1-methyl-3-trifluoromethyl-1*H*-pyrazole-5-boronic acid pinacol ester (24.3 mg, 0.0880 mmol), $Pd(Ph_3P)_4$ (8.5 mg, 7.4 μmol), potassium carbonate (0.073 mL, 0.15 mmol), and THF (1 mL) was heated at 100 °C for 1 h under microwave irradiation. The mixture was quenched with 0.02 M hydrochloric acid and extracted with AcOEt. The organic layer was separated, washed with brine, dried over $MgSO_4$, and concentrated under reduced pressure. The residue was purified by silica gel column chromatography (hexane/AcOEt = 40/60 to 0/100) and crystallized from AcOEt–$^iPr_2O$ to give the title compound as a white solid (22.2 mg, 0.0339 mmol, 46%). MS (ESI/APCI) *m/z* 655.3 $[M + H]^+$. ^1H NMR (300 MHz, DMSO-d_6) δ 3.18 (2H, t, *J* = 7.2 Hz), 3.26–3.38 (2H, m), 3.86–4.00 (5H, m), 4.37 (2H, t, *J* = 8.2 Hz), 6.31 (1H, s), 7.03 (1H, s), 7.37–7.46 (3H, m), 7.51 (1H, s), 8.79 (2H, s), 10.01 (1H, s). ^{13}C NMR (101 MHz, DMSO-d_6) δ 27.7, 37.5, 38.1, 45.5, 51.5, 104.6 (d, *J* = 2.2 Hz), 112.9 (t, *J* = 15.4 Hz), 113.1–113.4 (m), 114.4, 119.0, 121.4 (q, *J* = 267.8 Hz), 123.8, 126.8, 132.5 (t, *J* = 12.1 Hz), 134.5, 137.2, 139.6 (q, *J* = 37.4 Hz), 139.7, 140.2, 156.7,

157.7, 157.7, 158.9 (dd, J = 253.1, 5.9 Hz). Mp 156–158 °C. Anal. Calcd for $C_{26}H_{20}ClF_5N_8O_3S$: C, 47.68; H, 3.08; N, 17.11. Found: C, 47.55; H, 3.16; N, 16.88.

5.2. X-ray structure analysis

Crystal data for **27e**: $C_{26}H_{19}ClF_5N_7O_3S\cdot H_2O$, MW = 658.00; crystal size, 0.20 x 0.13 x 0.10 mm; colorless, block; triclinic, space group P-1, a = 9.15655(17) Å, b = 11.1562(2) Å, c = 13.4175(3) Å, α = 78.463(6)°, β = 89.913(7)°, γ = 84.381(6)°, V = 1336.25(6) Å^3, Z = 2, Dx = 1.635 g/cm^3, T = 100 K, μ = 2.767 mm^{-1}, λ = 1.54187 Å, R_1 = 0.038, wR_2 = 0.105.

All measurements were made on a Rigaku R-AXIS RAPID-191R diffractometer using graphite monochromated Cu-Kα radiation. The structure was solved by direct methods with SHELXS-97[30] and was refined using full-matrix least-squares on F^2 with SHELXL-97.[30] All non-H atoms were refined with anisotropic displacement parameters.

CCDC 1061355 for compound **27e** contains the supplementary crystallographic data for this paper. These data can be obtained free of charge from The Cambridge Crystallographic Data Centre via http://www.ccdc.cam.ac.uk/Community/Requestastructure/Pages/DataRequest.aspx?.

5.3. In vitro inhibitory activity against MGAT2

Protein preparation. The full-length coding sequences of human MGAT2 and mouse MGAT2 are identical to NCBI accession numbers NM_025098[6] and NM_177448,[31] respectively. All genes of interests were subcloned with FLAG tag in the N-terminal region into pcDNA3.3 vector (Life Technologies, Carlsbad, CA). The expression vector was transfected into FreeStyle293 cells (Life Technologies, Carlsbad, CA) for human and mouse MGAT2 expression. After 2-days-culture, cells were homogenized in ice-cold 20 mM Tris-HCl buffer (pH 7.5 at 25 °C) containing

1 mM EDTA and 300 mM sucrose. Total membrane fractions were isolated by ultracentrifugation. Pellets were re-suspended in the same buffer for each homogenization and stored at −80°C. The protein concentration was determined with the BCA Protein Assay Kit (Pierce Biotechnology, Inc., IL) according to the instruction manual.

RapidFire/MS assay. The test compounds were dissolved in 5 μL of an assay buffer, which consisted of 100 mM Tris-HCl (pH 7.5), 5 mM $MgCl_2$, 200 mM sucrose, 0.01% Tween 20, 2 mM DTT, 0.01% BSA, and 5% DMSO and incubated with 10 μL of 0.6 μg/mL MGAT2 enzyme for 60 min. The reaction was started with the addition of 5 μL of $^{13}C\times18$ oleoyl-CoA (Sigma-Aldrich, St. Lois, Missouri) and 2-oleoyl-glycerol (Sigma-Aldrich, St. Lois, Missouri) at 20 μM each. After incubation at room temperature for 30 min, the reaction was stopped with acetonitrile containing 0.88% formic acid and 1.3 μM 1,2-dioleoyl-glycerol (Sigma-Aldrich, St. Lois, Missouri) as an internal standard. High-throughput online solid phase extraction was performed using a RapidFire® 300 (Agilent Technologies, Santa Clara, CA). Mass spectrometric analysis was performed using an API-4000™ triple quadrupole mass spectrometer (AB SCIEX, Framingham, MA) in positive SRM mode. The SRM transitions for $^{13}C\times18$ dioleoylglycerol as a reaction product and dioleoylglycerol were set as 656.6/339.2 and 638.5/339.2, respectively. Analytical data was acquired using Analyst software version 1.5.0 (AB SCIEX, Framingham, MA) and 656.6/339.2 was divided by 638.5/339.2 for calibration. The IC_{50} values for test compounds were calculated using XLfit software (IDBS, London, UK).

5.4. In vitro inhibitory activity against DGAT1, DGAT2, and ACAT1

Protein preparation. The full-length coding sequences of human DGAT1, DGAT2, and ACAT1 are identical to NCBI accession numbers AB057815,[32] NM_032564,[33, 34] and NM_003101,[34]

respectively. All genes of interests were subcloned with FLAG tag in the N-terminal region to make expression vectors. Recombinant baculoviruses were prepared according to the procedure of the Bac-to-Bac baculovirus expression system (Life Technologies, Carlsbad, CA). After infection with recombinant baculoviruses, Sf-21 insect cells were homogenized in an ice-cold Buffer (100 mM sucrose, 50 mM KCl, and 40 mM KH_2PO_4/K_2HPO_4 at pH 7.4). Total membrane fractions were isolated by ultracentrifugation. Pellets were re-suspended in the same buffer for each homogenization and stored at −80 °C. The protein concentration was determined with the BCA Protein Assay Kit (Pierce Biotechnology, Inc., IL) according to the instruction manual.

Thin Layer Chromatography (TLC) assay. The assays with human ACAT1, human DGAT1, and human DGAT2 were performed by TLC assay. For human ACAT1 assay, 5 μM [1-14C]-oleoyl-CoA and 100 μM cholesterol were reacted with 30 μg/mL human ACAT1 enzyme for 40 min at 32 °C. For human DGAT1 and DGAT2 assays, 5 μM [1-^{14}C]-oleoyl-CoA and 40 μM 1,2-dioleoyl-glycerol were reacted with 30 μg/mL human DGAT1 and DGAT2 enzyme, respectively, for 40 min at 32 °C. The modified Bligh & Dyer method was applied to the sample preparations. Organic phase was applied onto a silica TLC plate (Merck KGaA, Darmstadt, Germany) and separated with a solvent system of hexane, ethyl ether, and acetic acid. The radioactivities incorporated into lipids were measured with Typhoon FLA 7000 (GE Healthcare UK Ltd, Buckinghamshire, England) and analyzed with Image Quant TL (GE Healthcare UK Ltd, Buckinghamshire, England).

5.5. Estimation of LogD at pH 7.4

$LogD_{7.4}$, which is a partition coefficient between 1-octanol and aqueous buffer pH 7.4, of the compounds was measured on the chromatographic procedure whose condition was developed

based on a published method.[35] The instruments were Waters Alliance 2795 HPLC system with 2996 UV-vis detector (Milford, MA, USA).

5.6. In vitro metabolic clearance in human and mouse hepatic microsomes

Human and mouse liver microsomes were purchased from Xenotech, LLC (Lenexa, KS). An incubation mixture consisted of microsomal protein in 50 mM KH_2PO_4–K_2HPO_4 phosphate buffer (pH 7.4) and 1 μM test compound. The concentration of microsomal protein was 0.2 mg/mL. An NADPH-generating system containing 5 mM $MgCl_2$, 5 mM glucose-6-phosphate, 0.5 mM β-$NADP^+$, and 1.5 units/mL glucose-6-phosphate dehydrogenase was added to the incubation mixture to initiate the enzyme reaction. The reaction was terminated 15 and 30 min after the initiation of the reaction by mixing the reaction mixture with acetonitrile, followed by centrifugation. The supernatant was subjected to LC/MS/MS analysis. The metabolic velocity was calculated as the slope of the concentration-time plot.

5.7. Pharmacokinetic analysis in mouse cassette dosing

Test compounds were administered intravenously (0.1 mg/kg) or orally (1 mg/kg, suspended in 0.5% methylcellulose aqueous solution) by cassette dosing to non-fasted mice. After administration, blood samples were collected and centrifuged to obtain the plasma fraction. The plasma samples were deproteinized by mixing with acetonitrile followed by centrifugation. The compound concentrations in the supernatant were measured by LC/MS/MS.

5.8. Evaluation of time-dependent inhibition (TDI) of CYP3A4 (single-point assay)

Human liver microsomes were purchased from Xenotech, LLC (Lenexa, KS). A mixture of a

test compound (30 μM) and microsomes in phosphate buffer (pH 7.4) was preincubated at 37 °C in the presence of an NADPH-generating system containing $MgCl_2$, glucose-6-phosphate, β-$NADP^+$, and glucose-6-phosphate dehydrogenase. After preincubation, enzymatic activity of CYP3A4 in the incubation mixture was determined by measuring 6β-hydroxytestosterone in the reaction with testosterone by UPLC. The activity (% of control) for each preincubation time was calculated to the following: {(activity with test compound)/(activity with DMSO)} ×100. The remaining activity (% remaining) after preincubation was calculated to the following: {activity with preincubation (% of control)}/{activity without preincubation (% of control)} ×100.

5.9. Evaluation of reversible inhibition of CYP isoforms

Human liver microsomes were purchased from Xenotech, LLC (Lenexa, KS). Inhibition activity of a test compound of each CYP isoform (1A2/2C8/2C9/2D6/3A4) was evaluated by incubating its specific substrate (tacrine/paclitaxel/tolbutamide/dextromethorphan/midazolam) with 0.1 mg/mL human microsomes in the presence of 10 μM test compound. The incubation mixture was allowed to stand for 10 min at 37 °C and then the incubation was terminated by addition of acetonitrile/water. After centrifugation, the supernatant was subjected to LC/MS/MS analysis to measure the peak of each specific metabolite (1-hydroxytacrine/6α-hydroxypaclitaxel/ 4-hydroxytolbutamide/dextrorphan/1'-hydroxymidazolam).

5.10. Phototoxicity test

BALB/c 3T3 cells were cultured at 37 °C, 5% CO_2 in DMEM supplemented with 10% fetal bovine serum, 50 IU/ml penicillin and 50 mg/ml streptomycin. Cells were seeded at 2.5×10^3 cells/well in 384-well white plate, and cultured in DMEM supplemented with 10% fetal bovine

serum, 2 mM L-glutamine, 1 mM sodium pyruvate, 50 IU/ml penicillin, and 50 μg/ml streptomycin for 1 day. Two 384-well plates per test compound (6.25 μM) in Earle's Balanced Salt Solution (EBSS) supplemented with 1 mM HEPES were preincubated for 1 h. One of the two plates was irradiated (+UV) for 60 min with 1.4–1.7 mW/cm^2 (5–6 J/cm^2), whereas the other plate was kept in the dark (−UV). In both plates the treatment medium was replaced by the culture medium and after another 24 h of culture the cell viability was determined by the cellular ATP content. The cellular ATP content was measured by Celltiter-Glo^{TM} assay kit (Promega) according to the manufacture's instruction. ATP content was calculated to the following. ATP content (% of control) = (RLU of test compound / RLU of 1% DMSO) × 100.

5.11. Oral fat tolerance test (OFTT)

Male C57BL/6J mice (20–25 g, Charles River Laboratories Japan, Inc.) were used in the OFTT study. The animals were fed with standard chow and tap water ad libitum, maintained at 23 ± 3 °C with a constant humidity of 40–70%, and acclimated with a cycle of 12 h of light and 12 h of darkness. All animal experiments were performed according to the guidelines of the Institutional Animal Care and Use Committee in Takeda Pharmaceutical Company Ltd. Overnight fasted mice were orally treated with a single dose of 0.3, 1, and 3 mg/kg body weight of compound **27c**. At 6 h after the treatment of **27c**, mice were orally given 8 mL/kg olive oil or water. To inhibit the hydrolysis of plasma TG by lipoprotein lipase (LPL), mice were treated with a LPL inhibitor, Pluronic F127 (Poloxamer 407, i.p., 500 mg/kg) 30 min prior to olive oil load. Blood samples were collected via tail vein at 0, 2, and 4 h after the olive oil load. Plasma fractions were obtained by centrifugation at 11,100 G for 5 min at 4 °C. Plasma TG concentration was determined using a 7180 biochemistry automatic analyzer (Hitachi high-Tech,

Japan). Chylomicron TG (CM/TG), a triacylglycerol derived from small intestine, was calculated by subtracting the plasma TG concentration of water-treated group from the plasma TG concentration of each olive oil-treated group.

Acknowledgements

We thank Dr. Minoru Sasaki and Dr. Rei Okamoto for compound synthesis and discussion about compound design, Yasumi Kumagai and Motoo Iida for structural determination by NMR experiments, Mitsuyoshi Nishitani for structural determination by X-ray crystallographic analysis, and Dr. Etsurou Watanabe for helpful suggestion on computational analysis. We also acknowledge Taisuke Mochida for preparing figures, the members in charge of determination of LogD value, CYP3A4 TDI evaluation, phototoxic test, DMPK evaluation, and elemental analyses.

References and notes

1. Yuan, G.; Al-Shali, K. Z.; Hegele, R. A. *Can. Med. Assoc. J.* **2007,** *176*, 1113.

2. Goldberg, I. J. *Biochim. Biophys. Acta* **2012,** *1821*, 719.

3. Nordestgaard, B. G.; Benn, M.; Schnohr, P.; Tybjærg-Hansen, A. *JAMA* **2007,** *298*, 299.

4. Harchaoui, K. E. L.; Visser, M. E.; Kastelein, J. J. P.; Stroes, E. S.; Dallinga-Thie, G. M. *Curr. Cardiol. Rev.* **2009,** *5*, 216.

5. Boullart, A. C. I.; de Graaf, J.; Stalenhoef, A. F. *Biochim. Biophys. Acta* **2012,** *1821*, 867.

6. Yen, C. L.; Farese, R. V., Jr. *J. Biol. Chem.* **2003,** *278*, 18532.

7. Cao, J.; Cheng, L.; Shi, Y. *J. Lipid Res.* **2007,** *48*, 583.

8. Yen, C. L.; Cheong, M. L.; Grueter, C.; Zhou, P.; Moriwaki, J.; Wong, J. S.; Hubbard, B.;

Marmor, S.; Farese, R. V., Jr. *Nat. Med.* **2009,** *15*, 442.

9. Nelson, D. W.; Gao, Y.; Spencer, N. M.; Banh, T.; Yen, C. L. *J. Lipid Res.* **2011,** *52*, 1723.

10. Tsuchida, T.; Fukuda, S.; Aoyama, H.; Taniuchi, N.; Ishihara, T.; Ohashi, N.; Sato, H.; Wakimoto, K.; Shiotani, M.; Oku, A. *Lipids Health Dis.* **2012,** *11*, 75.

11. Barlind, J. G.; Buckett, L. K.; Crosby, S. G.; Davidsson, O.; Emtenas, H.; Ertan, A.; Jurva, U.; Lemurell, M.; Gutierrez, P. M.; Nilsson, K.; O'Mahony, G.; Petersson, A. U.; Redzic, A.; Wagberg, F.; Yuan, Z. Q. *Bioorg. Med. Chem. Lett.* **2013,** *23*, 2721.

12. Scott, J. S.; Berry, D. J.; Brown, H. S.; Buckett, L.; Clarke, D. S.; Goldberg, K.; Hudson, J. A.; Leach, A. G.; MacFaul, P. A.; Raubo, P.; Robb, G. *Med. Chem. Commun.* **2013,** *4*, 1305.

13. Sato, K.; Takahagi, H.; Yoshikawa, T.; Morimoto, S.; Takai, T.; Hidaka, K.; Kamaura, M.; Kubo, O.; Adachi, R.; Ishii, T.; Maki, T.; Mochida, T.; Takekawa, S.; Nakakariya, M.; Amano, N.; Kitazaki, T. *J. Med. Chem.* **2015,** *58*, 3892.

14. Orr, S. T. M.; Ripp, S. L.; Ballard, T. E.; Henderson, J. L.; Scott, D. O.; Obach, R. S.; Sun, H.; Kalgutkar, A. S. *J. Med. Chem.* **2012,** *55*, 4896.

15. Biscoe, M. R.; Fors, B. P.; Buchwald, S. L. *J. Am. Chem. Soc.* **2008,** *130*, 6686.

16. Maiti, D.; Fors, B. P.; Henderson, J. L.; Nakamura, Y.; Buchwald, S. L. *Chemical Science* **2011,** *2*, 57.

17. NOE cross peaks were observed between H-4 (or H-6) on the pyrimidine ring and the methyl proton on the pyrazole 1-position.

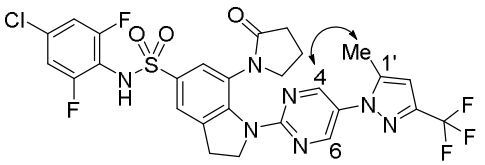

27f

18. Rietjens, I. M.; Vervoort, J. *Xenobiotica* **1989,** *19*, 1297.

19. Cnubben, N. H.; Vervoort, J.; Boersma, M. G.; Rietjens, I. M. *Biochem. Pharmacol.* **1995,** *49*, 1235.

20. Rietjens, I. M.; Vervoort, J. *Chem. Biol. Interact.* **1991,** *77*, 263.

21. Li, X.; Kamenecka, T. M.; Cameron, M. D. *Chem. Res. Toxicol.* **2009,** *22*, 1736.

22. Leeson, P. D.; Springthorpe, B. *Nat. Rev. Drug Discov.* **2007,** *6*, 881.

23. Nakashima, S.; Yamamoto, K.; Arai, Y.; Ikeda, Y. *Chem. Pharm. Bull. (Tokyo).* **2013,** *61*, 1228.

24. Stein, K. R.; Scheinfeld, N. S. *Expert Opin. Drug Saf.* **2007,** *6*, 431.

25. Ringeissen, S.; Marrot, L.; Note, R.; Labarussiat, A.; Imbert, S.; Todorov, M.; Mekenyan, O.; Meunier, J. R. *Toxicol. In Vitro* **2011,** *25*, 324.

26. Peukert, S.; Nunez, J.; He, F.; Dai, M.; Yusuff, N.; DiPesa, A.; Miller-Moslin, K.; Karki, R.; Lagu, B.; Harwell, C.; Zhang, Y.; Bauer, D.; Kelleher, J. F.; Egan, W. *Med. Chem. Commun.* **2011,** *2*, 973.

27. Dewar, M. J. S.; Zoebisch, E. G.; Healy, E. F.; Stewart, J. J. P. *J. Am. Chem. Soc.* **1985,** *107*, 3902.

28. Molecular Operating Environment (MOE), C. C. G. I., 1010 Sherbooke St. West, Suite #910, Montreal, QC, Canada, H3A 2R7, 2012.

29. Millar, J. S.; Cromley, D. A.; McCoy, M. G.; Rader, D. J.; Billheimer, J. T. *J. Lipid Res.* **2005,** *46*, 2023.

30. Sheldrick, G. *Acta Cryst. A* **2008,** *64*, 112.

31. Cao, J.; Lockwood, J.; Burn, P.; Shi, Y. *J. Biol. Chem.* **2003,** *278*, 13860.

32. Oelkers, P.; Behari, A.; Cromley, D.; Billheimer, J. T.; Sturley, S. L. *J. Biol. Chem.* **1998,** *273*, 26765.

33. Cases, S.; Stone, S. J.; Zhou, P.; Yen, E.; Tow, B.; Lardizabal, K. D.; Voelker, T.; Farese, R. V. *J. Biol. Chem.* **2001,** *276*, 38870.

34. Chang, C. C.; Huh, H. Y.; Cadigan, K. M.; Chang, T. Y. *J. Biol. Chem.* **1993,** *268*, 20747.

35. Masumoto, K.; Takeyasu, A.; Oizumi, K.; Kobayashi, T. *Yakugaku Zasshi.* **1995,** *115*, 213.

Figure 1. *N*-Phenylindoline-5-sulfonamide-based MGAT2 inhibitors.

Scheme 1. Synthesis of indoline-5-sulfonamide derivatives **9a** and **9b**[a]

[a]Reagents and conditions: (a) 4-chloro-2,6-difluoroaniline, 2,2,2-trifluoroethanol, MS4A, reflux; (b) Zn, AcOH, rt, 86% over 2 steps; (c) 4-chlorobutyryl chloride, DMA, 0 °C to rt; (d) NaH, DMF, 0 °C to rt, 91% over 2 steps; (e) NaOH, H_2O, THF, MeOH, rt, 87%; (f) 4-(trifluoromethyl)aniline, triphosgene, pyridine, THF, 0 °C; then **8**, TEA, THF, 0 °C to rt, 83%; (g) **11**, triphosgene, TEA, THF, 0 °C to rt; then **8**, THF, 0 °C to rt, 87%; (h) 2,2,3,3,3-pentafluoropropyl trifluoromethanesulfonate, TEA, THF, 0 °C to rt, 88%.

Scheme 2. Synthesis of indoline-5-sulfonamide derivatives **20a–c**[a]

[a]Reagents and conditions: (a) $Na_2S_2O_4$, EtOH, THF, H_2O, 60 °C, 73%; (b) 4-chlorobutyryl chloride, DMA, 0 °C to rt; (c) NaH, DMF, 0 °C to rt, 82% over 2 steps; (d) BnSH, $Pd_2(dba)_3$, Xantphos, DIEA, toluene, reflux, 96%; (e) NCS, AcOH, H_2O, rt, 81%; (f) 2-fluoro-4-(trifluoromethyl)aniline, 2,2,2-trifluoroethanol, 80 °C, 87%; (g) 2,4,6-trifluoroaniline, pyridine, rt, 70%; (h) H_2 (1 atm), Pd on carbon, THF, MeOH, rt, 93%–quant.; (i) **11**, triphosgene, TEA, THF, 0 °C to rt, 59–79%.

Scheme 3. Synthesis of indoline-5-sulfonamide derivative **23**[a]

[a]Reagents and conditions: (a) PhBr, RuPhos precatalyst, RuPhos, NaO^{t}Bu, DME, reflux, 65%; (b) NBS, DMF, 0 °C, 99%; (c) 4-(trifluoromethyl)phenylboronic acid, $Pd(PPh_3)_4$, K_2CO_3, THF, reflux, 63%.

Scheme 4. Synthesis of indoline-5-sulfonamide derivatives **27a–f**[a]

[a]Reagents and conditions: (a) 2-chloro-5-nitropyrimidine, THF, reflux, 98%; (b) H_2 (1 atm), PtO_2, THF, EtOH, rt, 93%; (c) *n*-pentyl nitrite, $CuBr_2$, CH_3CN, 0 °C to 60 °C, 45%; (d) $ArB(OH)_2$, $Pd(PPh_3)_4$, Na_2CO_3, THF/H_2O or DME/H_2O, 110–130 °C (microwave), 50–87% (for

27a and **27b**); (e) $ArB(OH)_2$, $Pd(PPh_3)_4$, K_2CO_3, THF, reflux, 38% (for **27c**); (f) substituted pyrazole, CuI, 8-quinolinol, K_2CO_3, DMSO, 130°C, 11–42% (for **27d**–**f**).

Figure 2. ORTEP of **27e**, thermal ellipsoids are drawn at 50% probability.

Scheme 5. Synthesis of indoline-5-sulfonamide derivative **34**[a]

[a]Reagents and conditions: (a) 2-chloroethyl isocyanate, cat. HCl, THF, 70 °C; (b) NaH, DMF, 0 °C to rt, 77% over 2 steps; (c) NaOH, H_2O, THF, MeOH, reflux, 92%; (d) 2-chloro-5-nitropyrimidine, THF, reflux, 92%; (e) H_2 (1 atm), PtO_2, THF, EtOH, rt, 97%; (f) *tert*-butyl nitrite, $CuBr_2$, CH_3CN, rt, 39%; (g) 1-methyl-3-trifluoromethyl-1*H*-pyrazole-5-boronic acid pinacol ester, $Pd(PPh_3)_4$, K_2CO_3, THF, 100 °C (microwave), 46%.

Table 1. MGAT2 inhibitory activity and CYP3A4 TDI profiles

[a] Inhibitory activity against human MGAT2. IC_{50} values are presented as means of duplicate experiments with their 95% confidence intervals in parentheses.
[b] CYP3A4 time dependent inhibition assay (n = 2). The remaining activity of CYP3A4 after preincubation with a test compound was determined.
[c] LogD value at pH 7.4.

Figure 3. Postulated mechanism of CYP3A4 inactivation

Table 2. MGAT2 inhibitory activity and CYP3A4 TDI profiles

[a] Inhibitory activity against human MGAT2. IC_{50} values are presented as means of duplicate experiments with their 95% confidence intervals in parentheses.
[b] CYP3A4 time dependent inhibition assay (n = 2). The remaining activity of CYP3A4 after preincubation with a test compound was determined.
[c] LogD value at pH 7.4.
[d] LLE = $pIC_{50} - LogD_{7.4}$.

Figure 4. Design stage from 1-carbamoylindoline derivatives to 1-arylindoline derivatives

Table 3. MGAT2 inhibitory activity and phototoxicity profiles

[a] Inhibitory activity against human MGAT2. IC_{50} values are presented as means of duplicate experiments with their 95% confidence intervals in parentheses.
[b] Phototoxicity assay using BALB/c 3T3 cell in the presence of 6.25 μM of compounds. Percentages of control are represented as means ± standard deviation (n = 3).
[c] The HOMO–LUMO energy gap (eV) of each simplified biarylaniline **I** calculated by AM1 method using MOPAC (**23-I**, **27a-I**, **27b-I**, **27d-I**, **27e-I**, **27f-I**, **27c-I**, and **34-I**).
[d] LogD value at pH 7.4.
[e] LLE = pIC_{50} − $LogD_{7.4}$.

Figure 5. Molecular orbital of HOMO and LUMO of compound **23-I** calculated by MOE (MOPAC, AM1).

Table 4. MGAT2 inhibitory activity, metabolic stability, and pharmacokinetic profiles

[a] Inhibitory activity against mouse MGAT2. IC_{50} values are presented as means of duplicate experiments with their 95% confidence intervals in parentheses.
[b]Human/mouse liver microsomal clearance. ND: The decrease of the compound concentration was not observed.
[c] 0.1 mg/kg, iv.
[d] 1 mg/kg, po.
[e] PAMPA permeability at pH 7.4.

Figure 6. Effect of **27c** on plasma TG elevation during oral fat tolerance test in C57BL/6J mice. **27c** (0.3, 1, 3 mg/kg) was orally administered 6 h prior to olive oil load. (A) Changes in plasma chylomicron/TG (CM/TG) levels after olive oil load. (B) Area under the curve (AUC) of plasma

CM/TG levels during 4 h after oil load. Data are the mean ± SD (n = 5). #, $p \leq 0.025$ versus vehicle by William's test.

Table 5. CYP3A4 TDI and reversible CYP inhibition profiles of **27c**

[a] CYP3A4 time dependent inhibition assay (n = 2). The remaining activity of CYP3A4 after preincubation with a test compound was determined.

A series of *N*-phenylindoline-5-sulfonamide derivatives was designed, synthesized, and evaluated as novel acyl CoA:monoacylglycerol acyltransferase-2 inhibitors for the treatment of obesity and metabolic disorders.

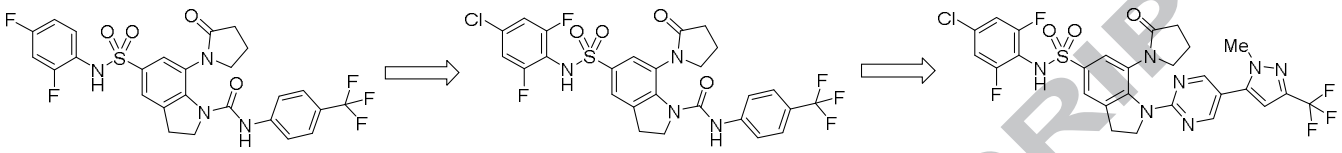

2
hMGAT2 IC_{50} = 3.4 nM
$LogD_{7.4}$ = 3.1
potenitial CYP3A4 TDI risk

9a
hMGAT2 IC_{50} = 30 nM
$LogD_{7.4}$ = 3.3
low CYP3A4 TDI risk

27c
hMGAT2 IC_{50} = 7.8 nM
$LogD_{7.4}$ = 2.8
low CYP3A4 TDI risk
BA 50% (mouse, 1 mg/kg)